Repeated movie viewings produce similar local activity patterns but different network configurations

Michael Andric[1] Susan-Goldin-Meadow[2], Steven L. Small[3], and Uri Hasson[1]
[1]Center for Mind/Brain Sciences (CIMeC), University of Trento, Trento Italy
[2]Department of Psychology, The University of Chicago, Chicago, USA
[3]Department of Neurology, University of California, Irvine, USA

Author copy of manuscript accepted for publication in *NeuroImage*

***Abstract*— People seek novelty in everyday life, but they also enjoy viewing the same movies or reading the same novels a second time. What changes and what stays the same when re-experiencing a narrative? In examining this question with functional neuroimaging, we found that brain activity *re*organizes in a hybrid, scale-dependent manner when individuals processed the same audiovisual narrative a second time. At the most local level, sensory systems (occipital and temporal cortices) maintained a similar temporal activation profile during the two viewings. Nonetheless, functional connectivity between these same lateral temporal regions and other brain regions was stronger during the second viewing. Furthermore, at the level of whole-brain connectivity, we found a significant rearrangement of network partition structure: lateral temporal and inferior frontal regions clustered together during the first viewing but merged within a fronto-parietal cluster in the second. Our findings show that repetition maintains local activity profiles. However, at the same time, it is associated with multiple network-level connectivity changes on larger scales, with these changes strongly involving regions considered core to language processing.**

Keywords*— *repetition, novelty, discourse, network-reorganization, inters-subject correlation, narrative

I. Introduction

The study of novelty remains a continuous interest in psychology and cognitive neuroscience. In modern cognitive psychology, an important early finding was that people show high sensitivity to novelty in an input series (Antrobus, 1968; Vitz, 1964). In neuroimaging, many studies have identified brain regions sensitive to novelty. Beyond those linked with memory systems per se (Ranganath and Rainer, 2003), fronto-parietal regions (Strange et al., 2005) and sensory systems (Brázdil et al., 2007; Liebenthal et al., 2003; Marois et al., 2000; Opitz et al., 2002) have also been shown as sensitive to the degree of novelty in an input. Novel stimuli can also induce network-level reorganization (den Ouden et al., 2010; Garrido et al., 2009; Kafkas and Montaldi, 2015). For example, unexpected changes in input predictability modulate changes in response coupling between specific sets of regions, suggesting reconfiguration in particular neural circuits (den Ouden et al., 2010). The degree of redundancy in an input has also been shown to impact whole-brain connectivity (Andric and Hasson, 2015).

The opposite of novelty is repetition. While there are clear indications that novelty brings on many changes, much less is understood about the potential impacts of repetition. The paradigmatic neurobiological model for studying repetition has been the repetition suppression paradigm (for initial review, see Grill-Spector et al., 2006). Such studies have shown that repeated processing of a stimulus results in reduced activity in brain regions involved in its initial processing. As already noted by Grill-Spector et al., repetition effects are "local" in nature: they are maximal in neurons most strongly responsive to the initial presentation, and they have a very rapid latency, consistent with an absence of top-down modulation. Neural-level models of repetition effects also emphasize local effects, assuming that repetition produces a reduction in the number of neurons involved (Brunet et al., 2014), reduced firing rates, or faster processing (Hawco and Lepage, 2014). In sum, many of results document local effects of repeated processing.

Beyond local effects, however, whether repeated processing involves macro-scale, or network-level, changes is unclear. Ewbank et al. (2013, 2011) found that repeated viewing of body parts modulates activity between regions involved in processing such stimuli, and suggested that repeated processing induces different interactions between regions. But, beyond their work, there is limited documentation of how repeated exposure to a stimulus impacts network-level brain activity. Importantly, no prior work has examined this question with respect to naturalistic stimuli.

At the neurobiological level, the issue of whether (and where) there are network-level changes to repeated exposures carries many possible implications. For example, clarifying this issue could help differentiate between networks whose organization is driven by stimulus characteristics and those whose organization is sensitive to prior experience. At the cognitive level, data of this sort could inform cognitive theories of repeated processing, which have long noted that re-experiencing does not necessarily produce a lack of interest. For instance, people can re-experience 'anomalous suspense'

This project was supported by European Research Council Starting Grant ERC-STG #263318 NeuroInt to U. H., and NIH/NIDCD Grant R01-DC03378 to Steven Small. Correspondence to andric.michael@gmail.com

when re-watching a thriller they had already seen and whose outcome is known to them (Gerrig, 1989). The fact that long-term knowledge of narrative outcomes does not necessarily interfere with the experience of suspense or enjoyment of narrative information suggests some independence, or even active disconnection, between the online processing of familiar information and long-term prior knowledge.

Our aim in the current study was to examine whole brain network-level reorganization during repeated viewing of naturalistic narratives. Neurobiological studies have not examined the neural correlates of re-experiencing narratives per se. However, there is work showing that, in certain brain regions, repeated viewing of a movie produces similar activity profiles across the two viewings on the local level – that of the single voxel. In a pivotal functional MRI (fMRI) study, Golland et al. (2007) presented participants with the same movie on two separate occasions. They found that occipital and lateral temporal regions (strongly linked to visual and language processing) showed similar activity patterns across the two sessions. In addition, that study identified a complementary set of regions with low correlation across the two viewings but strong correlations among each other. In other words, these complementary regions dissociated according to an intrinsic organization that was not driven by features of the external input. The authors thus suggested there exists an extrinsic brain network that strongly tracks external stimuli, as well as an intrinsic brain network whose activity is relatively input-independent. Further work using ECoG corroborated these findings by showing that electrodes recording from auditory and visual cortices tended to show similar gamma-band modulation profiles for initial and repeated movie viewing (Meshulam et al., 2013). The findings of these studies have particular importance for neurobiological theories of language and semantics. They suggest that activity in lateral temporal regions exhibit little, if any, impact of prior experience on activation patterns during stimulus processing.

Yet, external stimuli can impact brain activity during narrative comprehension not by altering activity patterns but by altering connectivity between brain regions. Chow et al. (2014) presented auditory stories to participants and found that connectivity of left inferior frontal gyrus (IFG) and left posterior middle temporal gyrus (MTG) with other brain regions varied depending on whether the story featured emotional, action, or perceptually vivid content. Wilkins et al. (2014) asked participants to listen to their favorite music, or other music they liked or disliked. They found that the global efficiency of connectivity of auditory cortex varied across conditions. In addition, the auditory cortex and hippocampus clustered together (i.e., were in the same "community") in the "like" and "dislike" conditions, but not in the "favorite" condition, in which the hippocampus appeared as an isolated community. Work by Muller et al. (2013) further suggests that familiarity impacts connectivity of auditory and medial temporal regions. In that study, the authors inserted periods of noise within familiar and non-familiar musical pieces. When noise was inserted within familiar music, participants were more likely to report the illusion of hearing music through the noise, and this was accompanied by stronger theta-band synchronization between right auditory cortex and right medial temporal lobe as measured via MEG and ECoG data.

Finally, in our own previous work, we presented participants with tonal series composed of four different tones that differed only in the regularity of the input series (Andric and Hasson, 2015). This manipulation induced different organization of whole-brain functional connectivity networks, impacting their modularity, the number of modules, node degree distributions, and partition structure. In addition, we observed a strong impact on the connectivity of lateral temporal regions involved in auditory and language comprehension. Specifically, we quantified the proportion of within-module functional connections maintained across listening to regular and random series and found that less than 30% of the connections in lateral temporal regions were maintained across the two conditions.

Taken together, these prior results for maintenance of activation patterns across repeated viewings (Golland et al., 2007) and context-dependent connectivity (e.g., Chow et al., 2014) suggest that lateral temporal cortices may exhibit two complementary features: i) on the local, micro-scale (that of single voxels), they would exhibit a relatively strong similarity between activation patterns during an initial and repeated viewing, whereas ii) on the larger macro-scale they would show a systematic shift in their network-level organization across viewings. In other words, we hypothesized that repeated exposure to a narrative produces "hybrid" reorganization, evident in a highly replicable response pattern on the scale of small brain regions, but accompanied by a significant level of reorganization at the network level. While these two features may appear, prima facie, incompatible, they are complementary. To illustrate, this would hold if a certain region (region A) responded identically to an initial and repeated presentation of a stimulus, but its activity might correlate with region B in the first exposure, whereas it would correlate with a different region (region C) during the second exposure.

To evaluate this question, we presented participants with identical audiovisual narratives produced by a single speaker in two viewings separated by a few minutes. To quantify the reliability of the response across viewings in different brain regions, we used an intra-subject correlation procedure (Golland et al., 2007; Levin and Uftring, 2001; Uftring and Levin, 2002) for identifying regions that responded similarly across the viewings. To quantify the reliability of the response across viewings in functional connectivity or network configuration, we treated each fMRI voxel as a node in a whole-brain network and established its connectivity to all other voxels in the brain (we generated these data for the first and second viewings). This derived a whole-brain network structure per participant per viewing, which allowed us to then compare functional connectivity metrics and network-level metrics across the viewings. We note that both types of analyses are within-participant analyses, only that the first examines the single-voxel level, whereas the second examines network-level features. Furthermore, we could evaluate whether individual differences in functional connectivity metrics correlated with differences in intra-subject correlations across viewings.

II. METHODS

A. Participants

Eighteen volunteers (11 women, M = 23.1 y.o.a, SD = 3.0) from the Purdue University community (West Lafayette, IN)

participated in the study. All were right handed (Oldfield, 1971), native speakers of American English, with normal hearing and vision, and without history of neurological or psychological disturbance. The Institutional Review Board of The University of Chicago approved the study. All participants gave written informed consent.

B. Stimuli

Participants were presented with seven video segments while undergoing fMRI (Figure 1). The videos presented a woman sitting on a chair and talking about various topics while being filmed in frontal view. These topics included (1) how to drive a car, (2) how to skate, (3) how to ride a bike, (4) how to use a pen, (5) the difference between a walk and a stroll and a shuffle, (6) how to swing a baseball bat versus swing a golf club, and (7) descriptions of string instruments (see Supplementary materials Table 1 for segment lengths). Though not instructed to do so, in all videos, the woman spontaneously produced co-speech gestures that accompanied her discourse. She did not receive prompting or instruction to make any gestures. The seven videos were each between 57 s and 166 s long (M = 126 s, SD = 39 s).

C. Procedure

Participants in the MRI scanner were presented with audio through ear buds and videos through goggles (NordicNeuroLab Audio/Visual system). The goggles were individually adjusted for each person. To make sure that participants could see and hear the video clips during the imaging session, we played a practice clip while the scanner emitted sounds heard during a mock functional scan and calibrated the audio level during this period. We told participants that they would be seeing a series of movies that show a woman discussing everyday topics. We instructed them to pay attention to the content and quality of the videos, while remaining as still as they comfortably could in the scanner. They were not told they would be seeing the same three runs twice in a row. We played the seven videos over three functional runs, with each run lasting 369 s. This was repeated a second time, for a total of six functional runs. Since the seven video clips were of different durations, we displayed black screen segments in between individual video clips to balance the total run times (Mean length = 28s, range = 11 to 47s). We presented two of the seven videos in each of the first two runs, and we presented the other three videos in the third run. Then we immediately repeated these three runs in the same order a second time. Thus, every participant saw each video twice. To avoid extra task demands, behavioral responses were not required from the participants while they were in the scanner.

Figure 1. Sample frames from videos. In all videos, the narrator explained simple concepts and gestured spontaneously without being instructed to do so. The narrator was the only person in the frame and the camera did not move.

To evaluate whether the participants were attentive during the imaging session, we administered a surprise 20-item multiple-choice questionnaire after participants exited the scanner. The questions required participants to recall specifics from the videos that would not have been answerable if they had not been engaged (for example, “Who tried to get Maggie to use figure skates?” “What kind of bike does Maggie say she has?”).

D. Image acquisition

We acquired scans using echo planar gradient echo T2* (blood oxygen level dependent; BOLD) imaging on a GE Signa Excite 3.0 Tesla scanner at Purdue University. We collected functional images across the whole brain, in the axial plane, using a 16 channel coil array under ASSET parallel acquisition with an acceleration factor = 2, TR = 1500 ms, TE = 26 ms, FOV = 20 cm, FA = 73 degrees, in 34 slices with thickness of 3.6 mm (no gap), and in-plane resolution of 3.125 x 3.125. We also collected a single high-resolution T1-weighted structural image per participant, using a TR = 5 ms, TE = 2.036 ms, FOV = 24 cm, FA = 12 degrees, in-plane resolution 256 x 224, for 166 sagittal slices of 1 mm thickness

E. Data analysis

1) Preprocessing

We processed participants’ functional time series for subsequent analyses in the following way. First, we discarded the initial four images of the time series, keeping data for which the BOLD response stabilized. We then removed respiration and cardiac pulse induced noise effects based on the RETROICOR method (Glover et al., 2000), implemented in AFNI (Cox, 1996). We applied this to the cardiac and respiration data collected during the imaging session. This method accounts for 13 respiration and cardiac related effects, on a slice-wise basis (including 4 regressors each for the cardiac and respiratory series and their harmonics, and 5 for the respiration variation of time and its harmonics). To account for motion during the scan, we registered time series images to the last image of the series. These registered images were then de-spiked, mean normalized to reflect percent signal change values, and de-trended to remove linear, quadratic, and cubic trends. We removed additional nuisance sources of variance from the time series by linear regression. This regression included predictors for scanner drift (linear, quadratic, and cubic) and motion parameters estimated during head motion correction. We also included predictors for high intensity white matter and low intensity ventricle signals. The white matter signal was obtained from an average of the upper quartile values in white matter voxels, and the low intensity ventricle signal from an average of the lower quartile values in ventricle

voxels. To increase the temporal signal-to-noise in each voxel's time series we applied 4 mm spatial smoothing. In addition, to accommodate the computational demands of our analyses, we resampled each participant's functional data to 4 x 4 x 4 mm. This resampling effectively reduced the number of voxels with functional data by about 45% as compared to the original resolution (3.125 x 3.125 x 3.6).

In this study, we were interested in cognitive processes taking place while participants were observing the movies; that is, the relatively high-frequency components associated with the phasic phase of movie viewing. To this end, we spliced together portions of the time series collected while participants observed the video clips and excluded those sections where there were intermediary blank-screen presentations between clips (1 blank screen in run1, 1 in run2, and 2 in run3). We also discarded data collected during the initial 6 s of each movie clip to mitigate onset-related effects associated with a shift from blank screen to movie presentation. This yielded 2 functional time series ("View1" and "View2") per participant, each with 547 functional images. Given the small number of splice points it is unlikely these introduced artificial correlations, but this procedure could have slightly reduced correlations driven by low-frequency fluctuations. Prior work has shown this procedure produces highly similar resting-state maps (Fair et al., 2007) under continuous acquisition, and we used it previously to document subtle contextual effects on connectivity during language comprehension (Hasson et al., 2009).

To limit the voxels analyzed to gray matter voxels, we created gray matter masks for each participant using FSL's bet for brain extraction (Smith, 2002) and first for segmentation (Patenaude et al., 2011). The gray matter mask was set to allow only voxels whose probability of being gray matter exceeded 33% This mask was defined after we had down-sampled the resolution of the data to 4 x 4 x 4mm. We only analyzed voxels in these masks. We aligned individual data to common MNI space using FSL's flirt (Jenkinson and Smith, 2001; Jenkinson et al., 2002) for registration of functional images to the high-resolution T1 images and then fnirt for non-linear alignment to MNI space (Andersson et al., 2007).

We created cortical surface representations of each participant's anatomy using FreeSurfer (Dale et al., 1999; Fischl et al., 2004, 2002, 2001, 1999a, 1999b). This inflated each hemisphere of the anatomical volumes to a surface representation that was aligned to a template of average curvature. We checked each participant's surface representations for any errors in the parcellation of white and gray matter surfaces after a first pass of FreeSurfer's recon-all program and corrected any errors on the surface. We used the 2-D surface space because it allows more accurate reflection of the individual data at the group level than the 3-D volume space (Argall et al., 2006). We thus conducted our voxel-wise similarity analysis (see Voxel-wise similarity below) in the surface domain. In this analysis, we projected each individual's community partitions to surface representations using SUMA (Saad et al., 2004) and then calculated partition similarity for each node. Due to computational demands, however, we could not conduct most of our analyses in this surface domain. For perspective, our individual masked gray matter volumes include 15,232 voxels on average, whereas a common group-level surface brain includes 392,004 nodes.

2) Intra-subject connectivity strength

To identify voxels that reliably tracked the movie features, we determined which voxels' time series showed significant correlations across the repeated viewings. We calculated intra-subject correlations (Pearson correlation coefficients) between the View1 and View2 time series for each participant (for the basis of this approach, see Golland et al., 2007; Levin and Uftring, 2001; Uftring and Levin, 2002). We applied Fisher's z-transformation to the correlations, which returned one value per participant per voxel. At the group level, we evaluated these correlation values by aligning them to a common MNI template using the transformations described in the section above, and then we performed a voxel-wise t-test against zero (the chance value). We identified significant clusters with a cluster-based control for family-wise error rate (FWE). We set the single voxel threshold at $p < 0.01$, with a volume of at least 1872 mm3 to control for FWE of $p < 0.05$. This value was determined using simulations, via AFNI's 3dClustSim, that took into account the data's estimated internal smoothing (~8 mm3).

3) Average connectivity-strength changes

Generating weighted-connectivity maps and differences across viewings

To examine voxel-level changes in connectivity strength, we used a voxel-wise connectivity measure (Cole et al., 2010). This measure (whole brain weighted global brain connectivity, or WGC) is the mean functional connectivity (as Pearson's R values, which were then Fisher's z-transformed) between each voxel and every other gray matter voxel. We create single-voxel WGC maps for the View1 and View2 data sets, yielding two whole brain (gray matter) maps per participant. To identify which voxels showed differences in mean functional connectivity across the two viewings, we compared these maps at the group level by paired-samples t-tests. We again used cluster-based control for FWE. We set the single voxel threshold at $p < 0.01$, again with a volume of at least 1872 mm3 controlling for a FWE of $p < 0.05$. Given a recent report of lack of control over FWE in these types of simulations (Eklund et al., 2016) we also repeated this analysis with a permutation-based method using FSL's randomise routine (Winkler et al., 2014), again using a cluster-forming voxel threshold of $p < 0.01$ and controlling for FWE of $p < 0.05$. The latter yielded a more conservative result, and we use that in the paper.

Quantifying whole-brain connectivity changes in voxels whose weighted-connectivity differed across viewings

As we detail in the Results, we identified a large perisylvian cluster in the left hemisphere, where voxels' whole brain WGC during the second viewing was stronger than the first. As a post hoc assessment, we wanted to understand which brain regions changed their connectivity with voxels in this cluster. However, given the functional heterogeneity of regions within this large cluster, we first evaluated to what extent this large perisylvian cluster could be partitioned into sub-clusters with different whole brain connectivity profiles during View2. Then, for each of these sub-clusters, we established its whole brain connectivity during View1 and View2 to identify areas showing significant differences at the group level.

We determined sub-clusters within the large perisylvian cluster as follows. For each participant, we performed

agglomerative clustering using Ward's criterion (Ward, 1963) on the View2 time series within the perisylvian cluster to obtain 4 sub-clusters. This clustering was based on the whole-brain correlation of each gray-matter voxel in that cluster. We chose 4 based on prior work arguing for separation of SMG, posterior STG, middle STG, and anterior STG functions (Boldt et al., 2013). This returned 4 clusters per participant. Then, to generate a group-level sub-cluster solution, we used the logic of a procedure introduced by Bassett et al (2013). We aggregated individual sub-clustering solutions across participants by constructing an "agreement matrix." This agreement matrix marked, for each pair of nodes (voxels) in MNI (group) space, the number of participants for which a pair of nodes belonged to the same sub-cluster. We treated the agreement matrix as weighted by proportion of participants in agreement at any one element and thresholded weaker elements as those with less than 30%, or 6/18 participants, following suggestions by Lancichinetti and Fortunato (Lancichinetti and Fortunato, 2012). From this agreement matrix, we then sought a consensus partition of the sub-clustering. We used the Louvain algorithm (Blondel et al., 2008) to determine an optimal partition from 50 runs of the algorithm (still following Lancichinetti and Fortunato, 2012). This yielded a consensus partition with 3 non-overlapping sub-clusters.

We transformed the locations of these 3 sub-clusters (roughly premotor cortex, posterior STG, mid-anterior STG) back into each participant's original space and derived a mean time series for each sub-cluster for the View1 and View2 time series. We treated these average time series as seeds and used them to construct whole brain connectivity maps. Note that the procedure for determining brain regions that show differences in whole brain connectivity between View1 and View2 is independent of the procedure used to define the clusters from which the time series were created (the latter were based on time series in View2 alone). On the group level, we then used paired-sample t-tests to identify areas whose connectivity with each seed region significantly differed for the View1 and View2 ($p < 0.001$ single voxel uncorrected threshold, $p < 0.05$ FWE controlled-for using cluster correction using permutation methods via FSL's randomise routine).

4) Topological connectivity measures

Generating connectivity matrices

We created a complete cross-correlation matrix from all voxels within a participant's gray matter for each participant. Across participants, the number of voxels in the masks ranged from 12873 to 16856 (M = 15232, SD = 1131). We binarized the connectivity matrices with an edge-density criterion (Alexander-Bloch et al., 2010; Ginestet et al., 2011) to maintain the same edge density (links) for all networks (i.e., networks for the 1st and 2nd Viewings for all participants). This makes the networks comparable in terms of size across conditions; a factor that needs to be controlled as it can impact network features in and of itself. We used edge density values of 5%, 10%, 15%, and 20%. We created these maps and performed subsequent analyses using a combination of Python, R, and functions from the brain connectivity toolbox (Rubinov and Sporns, 2010) in Matlab.

Node degree distributions

The degree of a node is defined as the number of edges (connections) in which it participates. We examined whether distributions of node degree values differed between View1 and View2 at each edge density level. Following previous studies (Achard et al., 2006; Andric and Hasson, 2015; Bassett et al., 2006; Fornito et al., 2010; Hayasaka and Laurienti, 2010), for each person's data in each of the two viewings, we fit the distribution of node degrees by a power law with exponential truncation:

$$P(k) \sim Ak^{\alpha-1}e^{k/k_c}$$

We then extracted values for the power law exponent (alpha), exponential cutoff point(k[c]), and coefficient (A), and evaluated these parameters at the group level using non-parametric tests for within-participant comparisons (Wilcoxon signed-rank test; due to non-normal distribution of the values tested).

Modularity

Modularity is a graph theoretic measure that can be used to evaluate the quality of a network partition. We applied this measure to determine an optimal partitioning of the networks for each participant's View1 and View2 connectivity matrices. The coefficient of modularity (Q) is higher the more partitioned a network is into modules. These modules can be recognized as densely intra-connected sub-networks. In other words, their connection densities are greater within modules than between them.

We applied this measure to the connectivity matrices with a fast unfolding community detection method (Blondel et al., 2008) that seeks to optimize modularity.

The modularity measure (Q) is given in Eq. (1):

$$Q = \frac{1}{2m}\sum_{C \in P}\sum_{i,j \in C}\left[Aij - \frac{k_i k_j}{2m}\right]$$

The indices i and j run over N nodes in the graph. A is the network adjacency matrix; m is the sum total number of edges; the degree of node i is $k = \sum_j Aij$; and the index C runs over the modules of partition P. This community detection algorithm seeks to maximize Q for a given network, with its optimized partition captured by the Q value.

We applied this algorithm to the binary connectivity matrices for each participant's View1 and View2 data. Given that this partition-finding algorithm is non-deterministic, we applied it 100 times to each network and chose the maximum Q value as representative of that View (i.e., condition) per participant at each level of edge density (Andric and Hasson, 2015; Stanley et al., 2014). In summary, this procedure provided a single Q value per network per participant, as well as a number reflecting the number of modules in the network. We then tested these values – modularity and module number – on the group level using a non-parametric test for within-participant comparisons (Wilcoxon signed-rank test).

As a validity check for the Q values we observed in the experimental data we also derived Q values from random networks. These random networks were created to match the number of nodes and degree-distribution in the experimental data, but with randomly assigned edges. We generated 100

random networks for each of the View1 and View2 data (per participant and edge density; i.e., n = 14400 random networks in total across viewings, participants, and edge densities). We performed this analysis on binarized networks at each of the density thresholds (5%, 10%, 15% and 20%).

Group-level modularity representation

To obtain a group-level partition structure reflecting the optimal modularity solutions of single participants, we again used the agreement matrix approach, following a similar procedure as outlined by Bassett et al (2013). We constructed an agreement matrix across participants that marked, for each pair of nodes (voxels), the number of participants for which this node-pair was in the same module after network partitioning. In our case, this meant that the minimum value for any one voxel-pair could be 0, and the maximum value could reach 18 (the number of participants). We applied this procedure to the partitions generated for View1 and View2. Note that we applied this procedure in common MNI space after transforming each participant's two partitions (View1 and View2) from original space to common space.

As shown by Bassett et al., these 'agreement' matrices can then be partitioned using usual partition finding methods. We therefore applied the modularity optimization to the un-thresholded agreement matrix. We performed this process 100 times and retained the solution at which Q was maximal. Thus, from this procedure, we derived two group-level partitions, reflecting the whole-brain organization for each viewing.

After obtaining these group-level partitions at each of the four different density levels we compared them across densities to assess which of the density thresholds was most representative (see Supplementary materials – Group-level modularity representation at different density thresholds). We determined that the 15% density threshold was most representative in terms of its partition structure, and we present results corresponding to this density threshold in further analyses.

Voxel-wise similarity

After obtaining each participant's optimal partition (as described in section 2.5.4.3), for each View1 and View2, we could determine for each voxel the extent to which its within-module connectivity cohort remained stable. Note that while this is a single-voxel (node) measure, it is still based on data obtained after partitioning the connectivity matrix into modules.

We used the Jaccard similarity coefficient (Jaccard, 1901) to assess the similarity of within-module connectivity sets in these two conditions, on a single voxel level. The Jaccard similarity coefficient is defined as the intersection of the two sets divided by their union, and yields a value between 0 and 1 at each voxel. Nodes that retained their within-module connectivity cohort across the two viewings obtain a higher value. We generated these voxel-wise maps for each participant. To generate a group map, we calculated the median value at each voxel across the individual-participant maps.

Aggregate dissimilarity tests

To obtain formal indicators for whether the group-level partition structures differed for View1 and View2, we used two tests, both using permutations. In the first, we built an expected similarity distribution (a sampling distribution), using a graph kernel based on the Weisfeiler-Lehman test of graph isomorphism (Shervashidze et al., 2011; see Vega-Pons et al., 2014 for previous application of this graph kernel with fMRI data; Weisfeiler and Lehman, 1968). This test iterates through the graphs and matches neighborhoods of nodes as subtree-like patterns. We first evaluated the degree of isomorphism that existed between the group-level View1 connectivity network and View2 connectivity network (generated as described in section 2.5.4.4). We treated these agreement matrices as graphs, keeping "strong" edges where at least 9 participants maintained a connection between nodes. This generated two 'binarized' group level adjacency matrices. We then applied the graph kernel to the adjacency matrices. We used the graph kernel over 2 iterations to derive a kernel matrix for the permuted graphs. We normalized the kernel matrix by [not shown] to yield similarity values between 1 and 0, corresponding to more and less similar. We refer to this measure as "W-L similarity."

We then implemented a permutation procedure to generate 'proxy' group-level View1 and View2 maps, and in each permutation we evaluated the similarity of the two group-level maps. This formed a sampling distribution against which to evaluate the value obtained for the real data. Each permutation proceeded as follows: we randomly selected a number of participants ($1 < n < 18$) only changing the label assignment of which partition solution was assigned to View1 and which to View2 on the single participant level. This reflected the null assumption that the group level agreement matrices for View1 and View2 are interchangeable across viewing condition. As above (section 2.5.4.4), we constructed group-level agreement matrices for each of these permuted sets, generating a proxy for the View1 group-level map and a proxy for the View2 group-level map. A W-L similarity score was derived for the permutation. We conducted 1000 permutations to construct a sampling distribution against which the real value could be compared.

We based the second test on a framework described by Zalesky et al (2010) for determining whether two connectivity matrices are significantly different. This test returns any connected graph component (whose extent exceeds chance) where the edges are more connected in one condition than another. We again implemented this procedure on the group-level 'agreement' matrices generated for View1 and View2. Recall that these matrices counted, for each voxel pair, the number of participants for which a given pair of nodes associated with the same module. We defined a 'significant difference' as one where this agreement score was equal to or greater than 9.

We again performed permutations to establish how many connected edges could be found this way by chance. Our permutation procedure followed the same approach as above to generate two agreement matrices ("proxy1" and "proxy2") per permutation. We then derived a single proxy matrix by subtracting the two matrices. From this single proxy difference matrix we computed the size of the largest component of connected edges that exceeded the value '8.' We performed 1000 such permutations. From this distribution, we determined that to control for alpha at $p < .05$ in our data, a component would need to be larger than 7057 voxels.

On the actual data, we performed a similar routine. We generated agreement matrices for View1 and View2, subtracted these matrices from each other and binarized their dissimilarity

by an absolute difference of at least 9. We then determined the connected components from this dissimilarity matrix and examined whether any exceeded the permutation-derived threshold of 7057.

5) Individual differences

We conducted several analyses targeting the correlation between accuracy on the behavioral task and our dependent neural measures. First, on the single-voxel level we tested for voxels/clusters where behavioral performance was related to intra-subject correlations (ISC) (as more attentive participants may perform better). Second, at the single-voxel level we further tested whether there were brain areas where behavioral accuracy correlated with weighted global connectivity (WGC) during the first viewing. We also we tested the relation between behavior and network modularity (Q) separately for the first and second viewing.

We also examined the relation between individual differences in ISC and WGC on the single voxel level. We defined two anatomical regions of interest in auditory and visual primary sensory regions (transverse temporal gyrus [TTG] and calcarine sulcus [CS]), and two in sensory association cortices (superior temporal sulcus and the anterior occipital sulcus, approximating human V5/MT+). For each region, we obtained the mean ISC in the region per participant. Because ISC profiles in the association cortices were highly correlated (Pearson's R = 0.73), we averaged those to obtain a single covariate for "higher-level" sensory regions. We then evaluated the association between WGC values and these three ISC covariates (TTG, CS, higher-level). Specifically, we conducted whole brain voxel-wise analyses examining the correlation between ISC and WGC in View1, between ISC and WGC in View2 and between ISC and the differences in WGC for View1 and View2 (deltaWGC = View1-View2). The correlations were Fisher's z-transformed, and all these analyses were corrected for multiple comparisons using family-wise error (single-voxel cluster forming threshold, $p < .01$, cluster-level correction, $p < .05$).

6) Time in scanner effects

Because the repeated presentations were presented later in the study we evaluated whether the experimental manipulation loaded on Time In Scanner (TIS) effects. Since our study consisted of three stimulus blocks both within the initial presentation and repeated presentation, we contrasted the third and first stimuli blocks (with each subset) to define a TIS contrast that is orthogonal to the repetition contrast (see Supplementary Figure 1 for graphical depictions of the repetition contrast and TIS contrast). We note that the interval between B3 and B1 (and between B3Rep and B1rep) was ~6.5 minutes, whereas the interval between the repetition set and initial set was ~10 min

III. RESULTS

First, we present results identifying which brain regions responded similarly on the single voxel level when the participants observed the same videos twice. Second, we present results that show where connectivity strength changed between the two viewings. Third, we describe network-level features of the functional connectivity patterns during View1 and View2.

A. Behavioral evaluation and relation to global connectivity or ISC

To make sure that participants paid attention to the videos they saw in the scanner, after exiting the scanner suite, participants were presented with a surprise 20-item, 4-choice multiple-choice questionnaire. This questionnaire asked them to recall specific details from the videos (e.g., "What kind of bike does Maggie say she has?"). Participants' mean accuracy on these questions was 87% (M = 17.39, SD = 2.09, range = 55% - 100%). This differs from chance (chance = 5/20; binomial test, $p < 0.0001$), indicating that participants were attentive to the videos.

As detailed in the Methods section, we aimed to identify regions where behavioral performance could relate to ISC (as more attentive participants may perform better). We did not find any. We also did not find brain areas where performance correlated with WGC during the first or second viewing. We also did not find a relation between behavior and network modularity (Q) for either the first and second viewing. A limited range in the behavioral responses could have narrowed our ability to identify such correlations: while the response-accuracy range was between 11 and 20 (out of a maximal score of 20), 84% of the participants had scores in the range of 16-19.

B. Intra-subject correlation: Areas that respond similarly across the two viewings

In this analysis, we identified brain areas by the systematicity of their responses in the two viewings (Figure 2). We correlated the time series of each gray matter voxel between the two viewings (an intra-subject correlation, Golland et al., 2007; Levin and Uftring, 2001; Uftring and Levin, 2002) and evaluated these on the group level (see Methods).

We identified widespread brain areas that responded similarly across the two viewings, and these findings matched well with those of Golland et al. (2007). These included occipital and lateral temporal areas implicated in auditory and

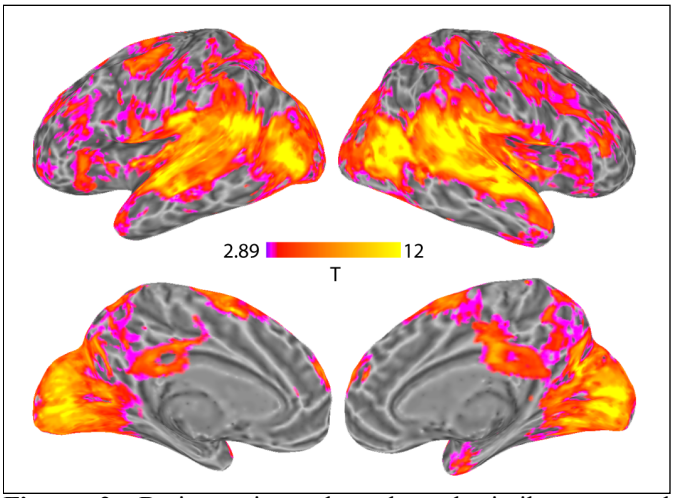

Figure 2. Brain regions that showed similar temporal response profiles across two movie viewings. Similarity was defined as the correlation between the each voxel's time series in the first and second viewing.

visual processing, the premotor cortex bilaterally (but not central sulcus) and the IFG bilaterally. We also found systematic responses in several main nodes of the default mode network, including the inferior parietal lobule and posterior cingulate (PCC) / precuneus bilaterally. Notable exceptions were the mid-anterior cingulate gyrus and ventromedial prefrontal cortex.

C. *Connectivity strength changes (global connectivity) across viewings*

For each voxel, we computed its mean connectivity value to all brain regions (weighted global brain connectivity, Cole et al., 2010), separately for the two viewings, and compared these values on the group level. We found significant connectivity strength changes – in all cases with stronger connectivity in View2 – in left lateral temporal cortex and adjacent supramarginal gyrus (Figure 3). No areas showed greater global connectivity for View1.

Note that areas showing global connectivity changes were, to a large extent, areas that also showed strong intra-subject correlations. As we elaborate in the Discussion, this means that these areas' connectivity with other brain regions increased from View1 to View2, despite showing similar local activity profiles across the two presentations.

1) Changes in functional connectivity of perisylvian regions

To better capture the nature of connectivity changes in the perisylvian cluster where whole-brain connectivity was greater during View2, we applied a clustering approach that partitioned this cluster into separate sub-clusters (on the group level). This produced three sub-regions of interest (see Figure 4A). The first region encompassed mainly SMG and postcentral gyrus (PoCG), the second encompassed middle parts of the superior temporal plane (STP), mainly over the transverse temporal gyrus (TTG), and the third was centered in a middle section of the STS.

We generated a whole-brain connectivity map for each of these (per participant, per View) to identify brain areas whose connectivity with these perisylvian sub-regions changed in View1 vs. View2. For the STS cluster (see Figure 4B), we found significantly stronger connectivity during View2 than View1 in superior central sulcus, parietal operculum, posterior and anterior STS (regions not included within the seed region), and extensive midline regions. For the STP cluster, we identified areas including right premotor, SMA, parahippocampal gyrus, parts of SMG bilaterally, and posterior cingulate gyrus. For the SMG/PoCG cluster, no clusters survived the threshold.

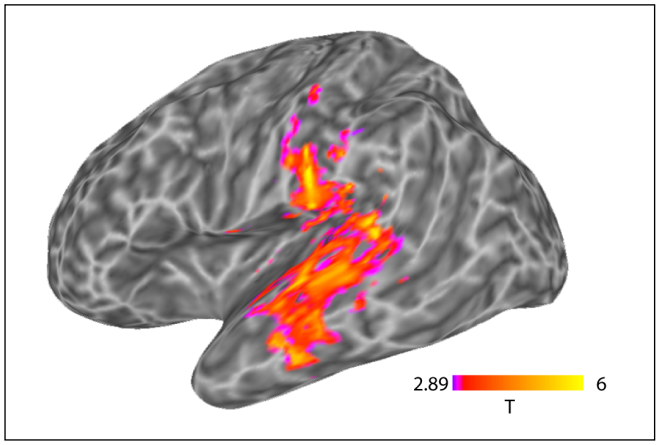

Figure 3. Brain regions whose mean whole brain connectivity was higher when viewing the movies for the second time.

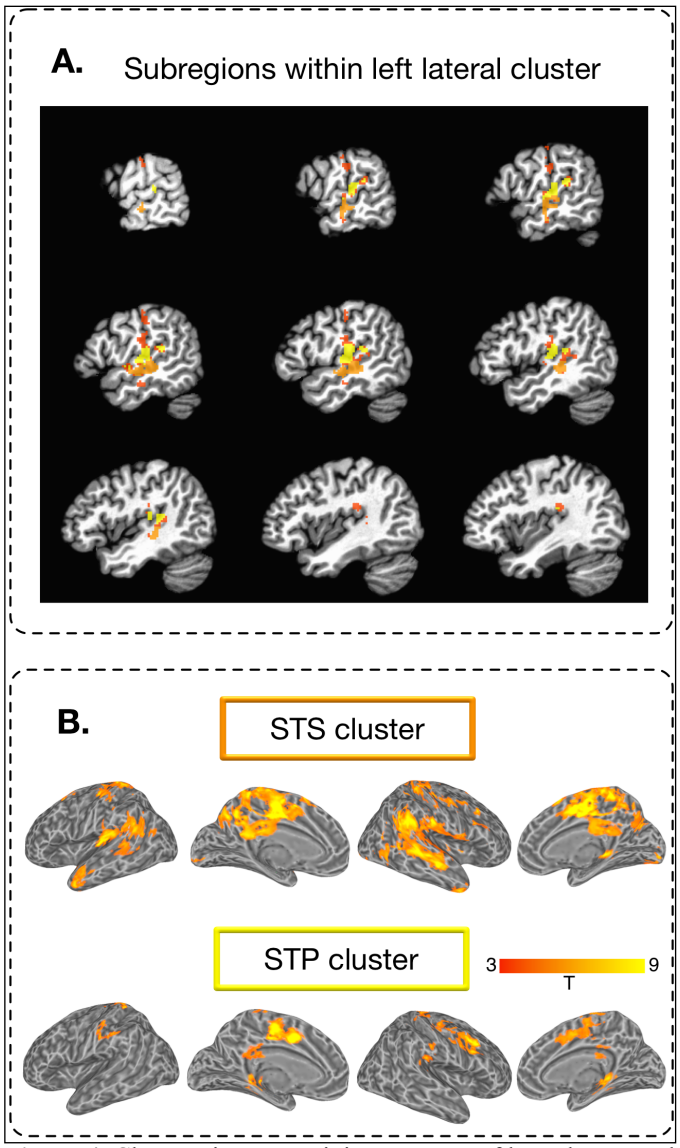

Figure 4. Changes in connectivity structure of lateral temporal cortex during second viewing. Panel A: Areas which showed stronger connectivity during the second viewing were partitioned to three separate sub-clusters: a superior cluster bordering SMG and PoCG (red), a central cluster in the superior temporal plane (STP; yellow) and an inferior cluster in STS (orange). Panel B: Brain regions that showed significantly stronger connectivity during View2 than View1 with the STP cluster and with the STS cluster.

2) Relation between global connectivity and intra-subject correlation

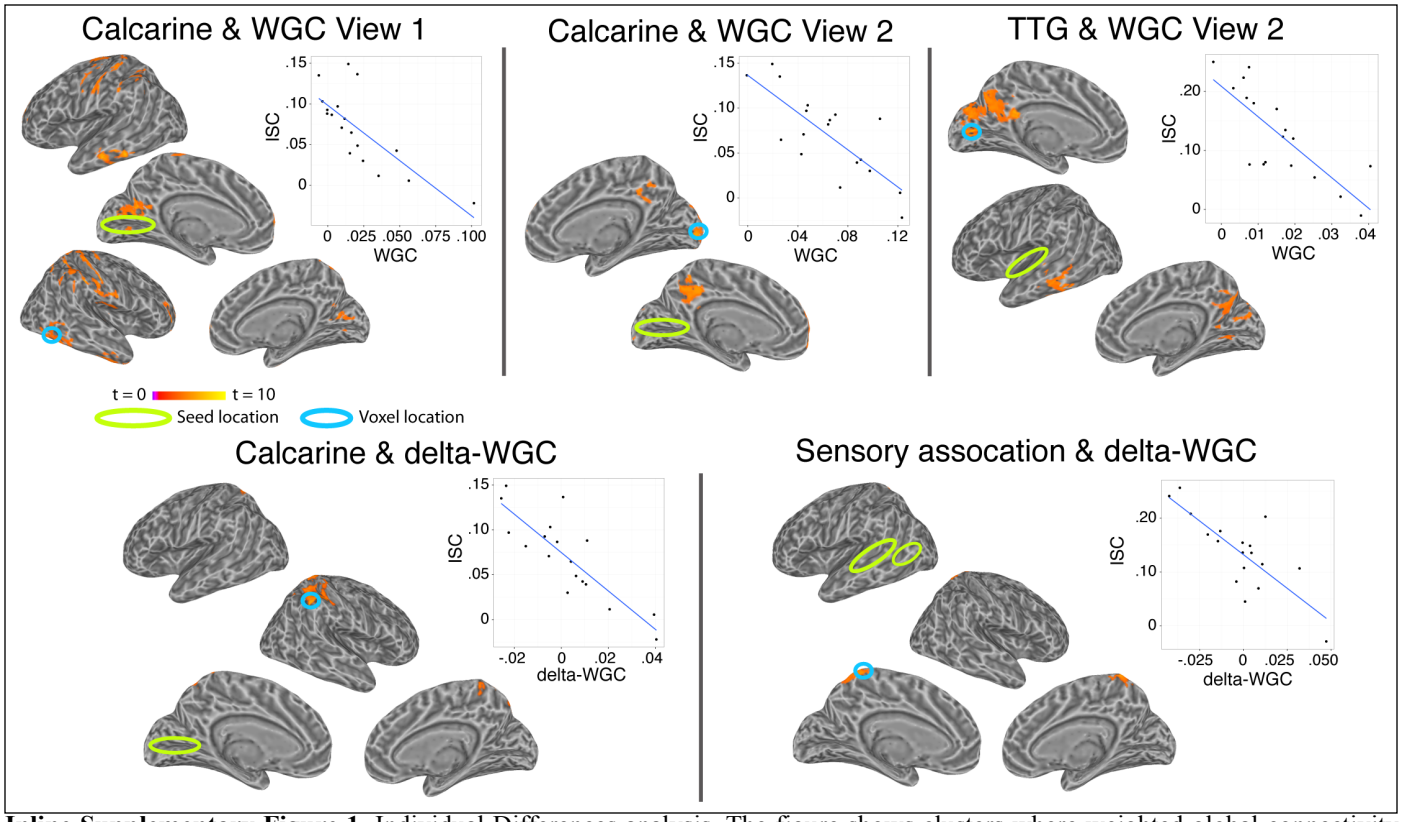

Inline Supplementary Figure 1. Individual Differences analysis. The figure shows clusters where weighted global connectivity (WGC) correlated with individual differences in magnitude of intra-subject correlations. Green circles mark the location of the cluster used for extracting ISC magnitudes, and blue circles mark locations of peak-voxels for which scatter plots are displayed. Upper row: areas showing ISC/WGC correlations during View1 or View2 for ISC patterns in Calcarine sulcus or Transverse Temporal Gyrus (TTG). Lower row: Areas where magnitude of ISC correlated with the difference between WGC in View1 vs. View2 (delta-WGC = View1-View2). ISC patterns in sensory association regions were themselves highly correlated and so were collapsed into a single measure.

We obtained ISC values for each person from the transverse temporal gyrus, calcarine sulcus and higher-level sensory association areas and evaluated whether they associated with WGC on the single-voxel level (see Methods). This analysis revealed interesting relations between the two metrics, summarized in Table 1 below. As Table 1 and Inline Supplementary Figure 1 show, higher ISC in lower level sensory regions (TTG, CS) was associated with reduced WGC values in numerous regions, during View1 and View2, and largely excluding sensory cortices themselves. For CS and the combined "associations regions" regressor, increased ISC was also associated with delta-WGC. However, these regions did not overlap with ones we reported as showing overall stronger WGC in View2 than View1. An examination of scatter plots for the ISC/delta-WGC correlation did not link higher ISC to stronger changes in WGC.

D. Topological organization of functional connectivity networks

1) Node degree distribution parameters do not differ

On the single participant level, for both View1 and View2, we found a good fit using an exponentially truncated power law to model the node degree distributions. Of three possible model forms (power law, an exponential, and an exponentially truncated power law), we found node degree distributions were best fit by the exponentially truncated model, with minimum Akaike Information Criteria values. Also, most participants' individual model fits exceeded an R^2 of 0.8 at every edge density for both View1 and View2. None of the parameter estimates, however, significantly differed between View1 and View2, at any edge density.

2) Modularity values and number of modules do not differ

Modularity did not differ significantly between View1 and View2 at any of the edge-density levels we examined (Inline Supplementary Figure 2A; Wilcoxon signed-rank tests; 5%: p = .45; 10%: p =.25; 15%: p = .17; 20%: p = .12). On the other hand, the observed Q values differed from Q values derived from random networks, with matching numbers of nodes and degrees (Wilcoxon signed-rank tests, all ps < 0.0005).

We also examined whether the number of modules differed between View1 and View2 (Inline Supplementary Figure 2B). Again, we did not find significant differences at any edge-density level (Wilcoxon signed-rank tests, 5%: p = .12; 10%: p = .11; 15%: p = .71; 20%: p = .38). To summarize, node degree distributions and modularity appeared to maintain across View1 and View2, but the network structure itself was more modular than would be expected by chance.

3) Two large-scale organizations for two viewings

We generated group-level network partitions reflecting assignment of voxels to modules, across participants, for View1 and View2. We generated these group-level partitions for different density thresholds (see Methods), but we focus on results obtained at the 15% density threshold, which best represented the data across densities (see Group-level modularity representation in the Methods section, and see Supplemental Materials for a table of similarity metrics and images across the other three density thresholds).

As shown in Figure 5, despite some similarity in the partition solutions during View1 and View2, there were important differences. First, we identified four modules for each viewing, but their composition changed in meaningful ways between viewings. For View1, we found a large module comprised of areas commonly implicated in language processing, including lateral-temporal cortex bilaterally, left IFG, and anterior aspects of the fusiform gyrus (reaching into the parahippocampal gyrus). This module's composition was absent in View2, which instantiated this module solely with inferior temporal areas, largely in the medial section of the parahippocampal gyrus. In View2, this "language-related" module seen in View1 largely merged with DMN areas, which in View1 held as a more typical DMN configuration (Figure 5, burnt orange in panels A, B).

Areas in lateral occipital cortex, notably the middle occipital gyri and right anterior occipital cortex (light green Panel A), including the most adjacent part of posterior middle temporal gyrus, were present in View1 in the aforementioned module that also contained lateral temporal and inferior frontal regions. By contrast, in View2, these areas merged with a module of areas that included premotor, motor, somatosensory, inferior parietal, and primary visual cortex (Figure 5, maroon in panels A, B).

Indeed, this largest partition of areas in View2 encompassed much of the premotor, motor, and parietal cortices, including the inferior parietal lobule (except the angular gyri, which remained part of the DMN in both viewings), intraparietal sulcus, and superior parietal lobule. It also includes the supplementary motor areas on the medial wall. Again, this subset included extrastriate visual areas in View2.

4) Network arrangement difference

We used two separate approaches to assess divergence between network arrangements found for View1 and View2. The first ("W-L similarity") used a graph kernel approach based on the Weisfeiler-Lehman test of graph isomorphism. The second examined whether there is a (larger than chance) connected set of edges that is more strongly connected in one of the conditions ("difference network"; Zalesky et al., 2010).

The graph kernel test indicated that the dissimilarity of networks structures between View1 and View2 exceeded chance ($p < .01$ see Inline Supplementary Figure 3). The second, "difference network" test identified a large difference component that consisted of 8432 voxels. Based on permutations, the probability of finding such a large cluster by chance was well below 1%, $p < 0.005$. Details of the network features of this "difference network" are shown in Inline Supplementary Figure 4. The vast majority of nodes involved in the difference network only had 1 or 2 connections, and only about 10% of the values exceeded 10. A truncated power law fit this degree distribution better than a power law (log likelihood ratio 43.7, $p < 0.0001$). Moreover, the higher degree valued nodes (i.e., those more connected in the difference network) dispersed in areas throughout the brain, including lateral and inferior temporal, frontal, and posterior medial cortices.

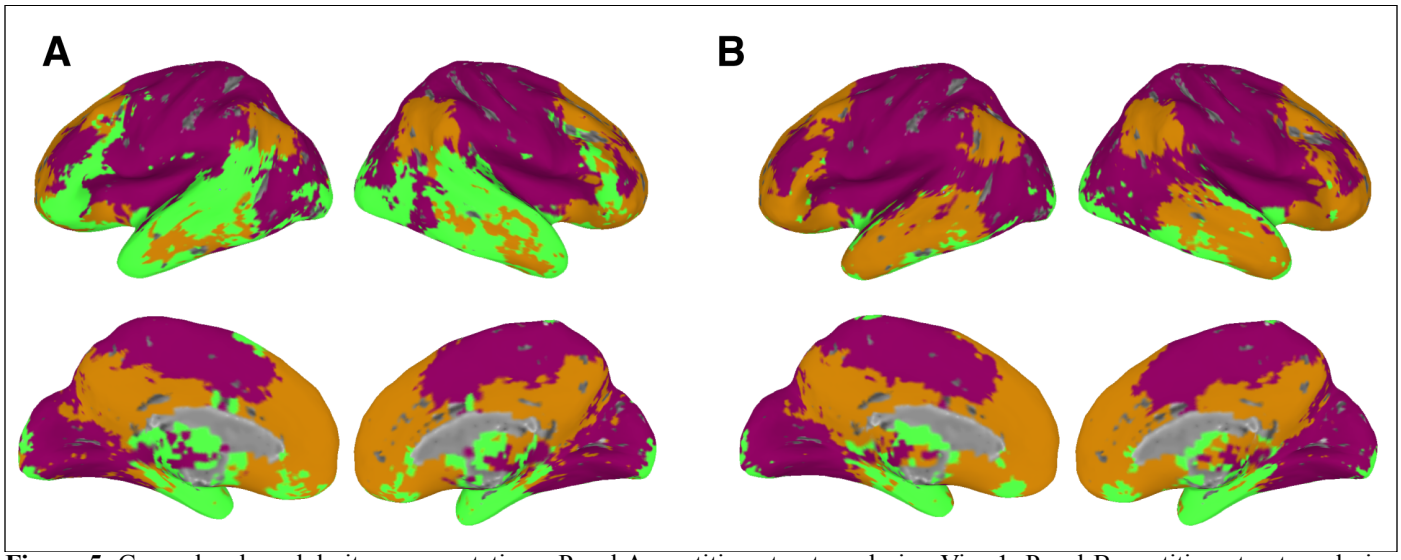

Figure 5. Group-level modularity representations. Panel A: partition structure during View1. Panel B: partition structure during View2. Within each view, each module is represented by a separate color. We maintained colors across views to highlight similar modules. As can been seen, view1 includes a large module comprising lateral temporal and inferior frontal cortices. In View2 however, this module merges with what in View1 was a module of Default Mode regions.

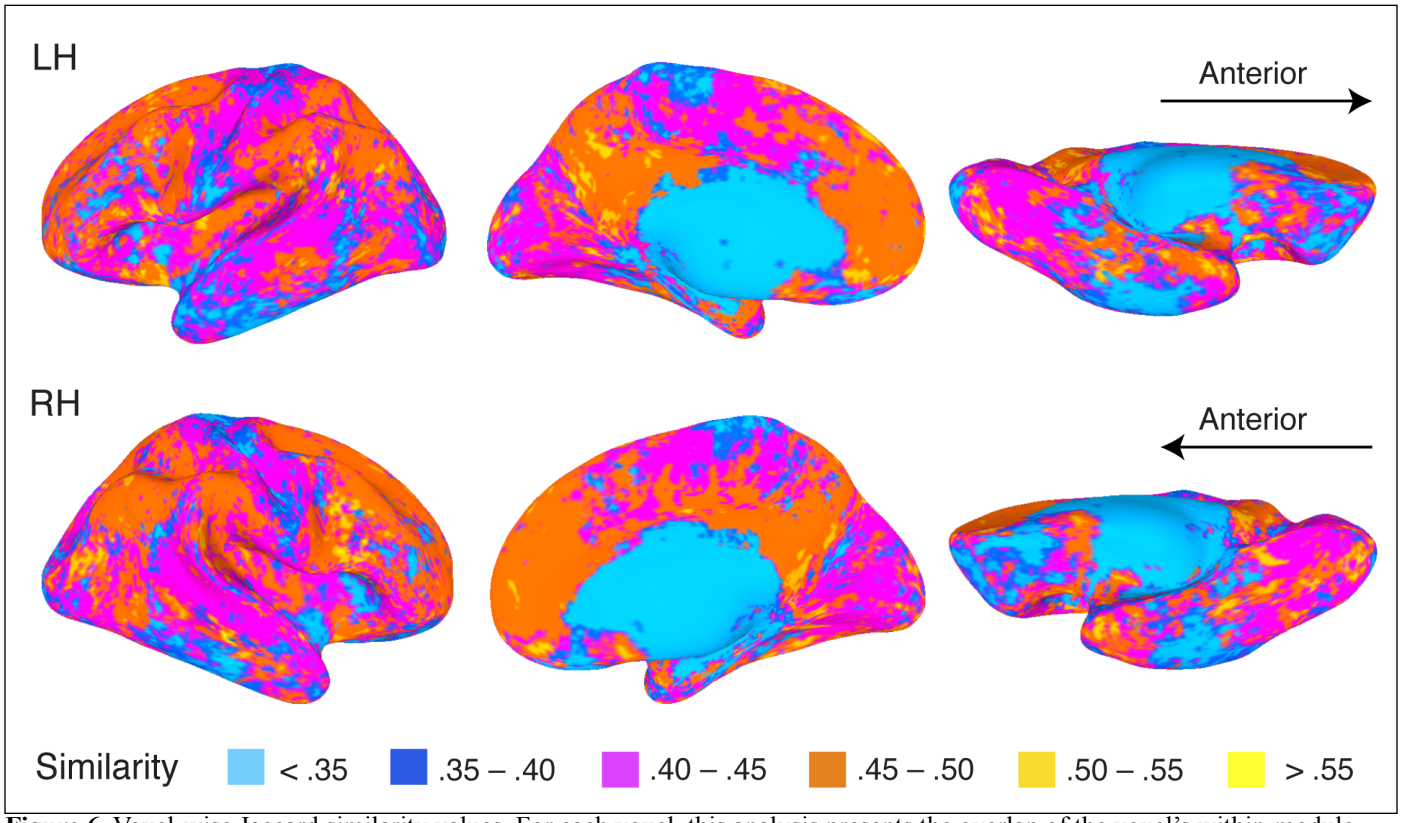

Figure 6. Voxel-wise Jaccard similarity values. For each voxel, this analysis presents the overlap of the voxel's within-module connectivity sets. Similarity was strongest in Default mode brain regions, but weaker in lateral temporal regions.

5) Similarity of within-module connectivity at single node level

After obtaining the optimal partition for each of the two viewings per participant, we determined, for each voxel, the overlap of its within-module connectivity cohorts in the two conditions (using the Jaccard similarity coefficient; see Methods). Because this procedure was performed after finding an optimal partition, and given the reliance of the latter on the density use to threshold connectivity matrices, we computed the Jaccard coefficient for each density separately but focused on the 15% density threshold as explained above. Figure 6 shows the resulting map for the 15% density threshold.

As can be seen in Figure 6, voxels within the DMN tended to maintain within-module connections across the two viewings (see Andric and Hasson, 2015 for similar results in a different paradigm). By contrast, values for lateral temporal cortices, bilaterally, as well as left IFG were lower. In other words, these language-related areas were ones whose within-module connections were more susceptible to change between View1 and View2.

E. Time-in-scanner effects

Given that the repeated viewing occurred later in the scanning session we evaluated an orthogonal control for Time In Scanner effects that was orthogonal to the repetition contrast (see Methods 2.5.6). For changes in weighted global connectivity (as reported in Section 3.3) we found no effects in cortical regions. For the difference network analysis (as reported in Section 3.4) we also found a null effect. The actual partition structure for the networks created from Blocks 1, 4 and Blocks 3,6 were highly similar as opposed to what was shown in the repetition contrast (Figure 5). However, the results of the within-module connectivity at the single level did reveal similar results to that seen in Figure 6, indicating more consistent within-module connectivity in DMN regions than in perisylvian ones.

IV. Discussion

Much recent interest surrounds the relative flexibility of brain networks to reorganize given stimulus properties or context (e.g., Alavash et al., 2015; Andric and Hasson, 2015; Bassett et al., 2013, 2011; Moussa et al., 2012). In this study, we examined the strength and topology of reorganization as a consequence of simply re-watching audiovisual narratives discussing everyday topics. On the local-level (of voxels), our functional connectivity analyses showed stronger global brain connectivity during the second viewing in three regions: two focal clusters in the cingulate motor region and amygdala, and one large cluster encompassing several left perisylvian regions. Interestingly, these same perisylvian regions also showed high similarity in their time series fluctuations across the two viewings. This shows that organization is dependent on spatial scale – during repeated processing certain brain regions maintain their local response profile, while at the same time substantially changing their connectivity structure.

On a larger scale – that of the whole brain – we found that re-viewing induced different clustering partitions of functional connectivity data. Notably, changes in the clustering of regions

within modules were most salient in lateral temporal and inferior frontal regions linked to language processing, and in regions associated with biological motion processing (lateral occipital to posterior temporal pathway). Changes in connectivity in this latter pathway are likely because of extensive use of gestures by our narrator. What is important is that those brain regions most implicated in processing the stimulus did not maintain their connectivity structure but instead were among the regions that showed the strongest alteration in connectivity structure. We also found that the functional networks differed significantly, as quantified by two measures: the isomorphic dissimilarity of the networks and a voxel-level index of partition changes across viewings. However, core topological features, including modularity and node-degree distributions, did not vary across viewings. This suggests no fundamental reorganization in the brain's capacity for information transfer between sub-networks.

Thus, perceiving the same content in different contexts – here, a first and second viewing – induced macro-scale reorganization of functional networks while sustaining highly similar activity patterns at the local level. In what follows, we discuss these findings in relation to the existing literature and their implications for future work.

A. The impact of context on strength of functional connectivity and reliability of activation

We examined functional connectivity strength with two aims in mind. First, we sought to identify brain regions whose time series showed high similarity across the two viewings. Second, we sought to identify whether (and if so, where) global brain connectivity (Cole et al., 2010) differed across viewings. As we highlighted in the Introduction, prior studies have documented similarity in local responses between repeated stimulus exposures. But whether the areas showing these local responses can, at the same time, reorganize in terms of their functional connectivity was unknown.

Using an intra-subject analysis (Golland et al., 2007; Levin and Uftring, 2001; Uftring and Levin, 2002) we identified extensive parts of occipital, temporal and frontal cortex with strong intra-subject correlations across the two viewings on the single voxel level. The spatial extent of these effects extended beyond low-level sensory cortices, indicating sensitivity to higher-level features of the input across viewings.

At the same time, some of these same regions, particularly within a large cluster of left perisylvian regions (SMG, STG, mid-STS), showed higher WGC in the second viewing than in the first. To understand this increase in correlation strength, we partitioned this large cluster into sub-regions. We determined three sub-clusters: 1) an STS cluster, 2) a superior temporal plane (STP) cluster, around TTG/TTS, and 3) a cluster that was predominantly superior to these, in the PoCG and parietal operculum. This functional subdivision is consistent with that found in prior work on naturalistic language comprehension (Boldt et al., 2013).

For each of these sub-clusters we then determined which brain regions correlated more with it during the second viewing than during the first. For the STS cluster, in the left hemisphere we found stronger connectivity with motor regions in the central sulcus, a middle cingulate region, the PCC, precuneus, the posterior part of the sylvian fissure, the parietal operculum, and left temporal pole. On the right, stronger connectivity extended even more, including SMA, precuneus, PCC, the parahippocampal gyrus, STG, and a large section of STS, while also including the temporal pole. For the STP cluster we found fewer regions. On the left, we identified the middle cingulate cortex. On the right, stronger connectivity included the precentral gyrus, SMA, and parahippocampal gyrus. Thus, lateral temporal regions generally showed greater connectivity to posterior association cortices during the second viewing.

The stronger connectivity of the left STS region with SMG bilaterally, extensive parts of right STS as well as the temporal poles bilaterally shows that a repeated viewing produces stronger connectivity between left STS and core regions linked to language processing. In addition, stronger connectivity with the right parahippocampal gyrus accompanied this. Taken together, these areas' increased connectivity makes plausible that prior knowledge of the communicated content allowed greater synchronization within these language-associated areas. This could be due to reduced low-level processing related to interpretation of the speech signal itself.

The STP region also showed stronger connectivity during repeated viewing but with many regions whose function in language typically associates with sensory-motor aspects of (sub-lexical) speech processing at the phonetic level. These regions included right precentral gyrus, left post-central gyrus, right parietal operculum, and primary and supplementary motor areas in the midline aspect of the brain (see Skipper et al., 2007 for related findings). Interestingly, prior work documented stronger connectivity within a similar network, involving posterior superior temporal, premotor, and M1-S1 areas during imitation than observation of audiovisual syllables in healthy adults (Mashal et al., 2012). It may be that prior knowledge of the spoken materials also leads to better coordination between the 'motor' (dorsal stream of speech perception; Hickok and Poeppel, 2007) and 'auditory' regions mediating sub-lexical speech perception. This finding is important because much of the work on the motor system's involvement in speech perception derives from assessments of activation magnitude in different conditions. By contrast, our paradigm relied on temporally extended observation (listening) conditions, and provides insight about superior temporal plane connectivity from a unique perspective.

We did not anticipate increased connectivity with the cingulate cortex, since this region is not typically implicated in language comprehension. The section of this region that showed increased connectivity matches a well-defined anatomical subsection of the cingulate gyrus, identified via resting state (Yu et al., 2011), DTI and cytoarchitectonic studies (Brodmann areas p24a', p24b', 24dv, 24dd). Focal activations of this cingulate sub-region have been linked with processing language and action information (Torta and Cauda, 2011). Indeed, our stimuli presented conversational narratives, including the speaker's ongoing use of co-speech gestures. It may then be that this region plays an important role in narrative comprehension (Ferstl et al., 2008), perceiving actions that co-occur in social communication (Mainieri et al., 2013) or interpersonal communication (Stephens et al., 2010), more generally. Nonetheless, this region's role in such contexts requires further study.

Finally, we identified several areas where individual differences in the strength of ISC correlated with WGC during View1 and View2. For the TTG seed region, increased ISC was

associated with decreased WGC in PCC/Precuneus bilaterally, left MTG and the calcarine sulcus during View2. For the calcarine seed, we found negative correlations during View1 in precentral/postcentral gyri bilaterally, and in the calcarine sulcus itself, meaning that greater calcarine ISC was linked to reduced connectivity of the region itself. In View2, we also found negative correlations for PCC/Precuneus.

This link between ISC and WGC in PCC/Precuneus suggests there is a relationship between externally-oriented ("extrinsic") computations and the connectivity a core node in what has been termed an "Intrinsic" system. Taking ISC as an indicator of (passive) monitoring of the external environment, our finding constitutes a strong, ecologically valid, indicator that connectivity within the DMN does relate to engagement with external stimuli. This has been shown in prior work by linking connectivity of the network to task performance demanding executive function (Hampson et al., 2006; Weissman et al., 2006) or to correlations with the task-positive network (Kelly et al., 2008). Other work has linked performance on tasks that demand executive function to task-induced network reconfiguration (e.g., Alavash et al., 2015; Bassett et al., 2011). Our manipulation is clearly of a different type, as participants were not engaged in any overt task that demanded executive function. We found that parietal regions (both superior and inferior) showed a relationship between ISC and delta-WGC, with the modal pattern being higher WGC in View2 for participants with higher ISC. In fact, this pattern was evident as a trend when observing the entire-group data (as opposed to a few outlying participants). We found that participants with highest ISC showed greater WGC in View2 than in View1 and participants with lowest ISC showed lower WGC in View2 than in View1. This suggests that individual differences in how people monitor external stimuli might express themselves as weighted shifts among connectivity relations rather than outright differences in the magnitude of change.

B. The impact of context on network modularity and partition structure

Our analysis of weighted global connectivity and the follow-up analyses examining differences in correlation strengths (section 4.1) are methods for analyzing functional connectivity that operate at a different scale than analyses based on network partitioning, and that assess a different aspect of connectivity. For instance, two networks may differ by functional connectivity strength yet have the exact same partition structure. This could be the case if a similarity measure (e.g., a correlation coefficient) between each pair of regions increased by a constant. We thus examined connectivity not only by its strength of similarity across viewings, but also by its macro-scale organization via characteristic network partitions.

By considering each voxel as a node in a functional connectivity network (Andric and Hasson, 2015; Hayasaka and Laurienti, 2010; Moussa et al., 2012) we derived functional connectivity maps with high spatial resolution and evaluated their network features using graph kernel and network difference methods. The graph kernel-based analysis (Shervashidze et al., 2011) showed above-chance dissimilarity in a test of the isomorphism between networks, represented as graphs. Given that the graph kernel we used quantifies each node's neighborhood connectivity, this difference means there are systematic differences in nodes' 'local' organizations across viewings. The network difference analysis (Zalesky et al., 2010) determined a large component within the difference network between the two viewings, with diffuse distribution of nodes over the entire cortex. Thus, on these metrics, the two whole-brain networks were found to differ substantially.

In prior work, we found that contextual manipulations can impact core topological features of whole brain networks, such as their modularity or node-degree distributions (Andric and Hasson, 2015). But this was not the case here. Instead, these core metrics held between viewings. Thus, at least at the level of their abstract topology, the networks were comparable. While it is difficult to argue from a null result, due to the within-subject design, the variance of these parameters (error bars in Inline Supplementary Figure 2) was extremely small, allowing ample power to identify differences in these metrics if they existed.

At the same time, the spatial organization of the partition structure differed across viewings. From the perspective of language comprehension and processing of meaningful biological motion, two notable differences emerged. First, perisylvian regions associated with language comprehension (lateral temporal cortex bilaterally and IFG bilaterally) comprised a distinct module during the first viewing (green, Figure 5) but not the second, where they merged into a larger module containing many association cortices. Furthermore, during the first viewing this "language" module also included regions associated with a functional pathway through middle occipital, lateral occipito-temporal (and MT/V5) and adjacent posterior middle temporal cortex. These latter regions are very often implicated in processing biological motion and audiovisual speech comprehension (Andric and Small, 2012; Andric et al., 2013; Bernstein and Liebenthal, 2014; Peigneux et al., 2000). In the second viewing, however, these regions also diverged into different modules. Notably, right middle occipital gyrus and anterior occipital sulcus shifted from clustering with "language" regions into a cluster with primary occipital cortex, inclusive also with motor, somatosensory, and parietal cortices (maroon, Figure 5). To summarize, higher-level auditory and association cortices linked to biological motion processing did not maintain their modular structure, merging into larger modules on the second viewing.

Such shifts in the grouping of regions within modules were not the rule. For instance, large parts of cortex recognized as part of the default mode network (DMN; IPL, SGF, PCC/Precuneus, ACC and inferior temporal cortices) were assigned to a single module in both viewings (burnt orange, Figure 5). Likewise, most of motor and somatosensory cortices (both laterally and medially), as well as medial occipital cortices, maintained a module identity across viewings.

We also examined the impact of module partition reorganization (across viewings) at a voxel-level resolution. For each voxel, we quantified the similarity of its within-module cohort across the two viewings. The group-level result showed that voxels in the DMN, as a whole, maintained the highest proportion of their within-module cohort, whereas lateral temporal regions exhibited much lower values (Figure 6; see Andric and Hasson, 2015 for similar findings). This sort of heterogeneity in stability of functional connectivity with context corroborates prior work (Mennes et al., 2013) that found that DMN regions tended to maintain their connectivity

patterns under different tasks, and that sensory cortices were more likely to change these patterns. Changes in within-module connectivity were also found for lateral occipital-temporal areas, as well as the medial occipital cortex (Figure 6). The latter result is notable because it provides a point of possible differentiation from the group-level modularity solutions. Recall that medial occipital cortex, including V1, showed a common clustering across the two viewings (Figure 5). However, the results of this voxel-level analysis indicate, even within that region, voxels tended to substantially shift their within-module connectivity pattern. We note that similar progressions of shifts in connectivity were also identified in the Time in Scanner analysis, though the latter analysis revealed null effects for the other tests used in this study. This may suggest that the result of consistency at the single-node level reflects a mixture of time-in-scanner and repetition effects.

It is interesting that all these changes occurred with no observable changes to the actual topological features of the network (modularity, module number, parameters of node degree distributions). This demonstrates that even though the latter indicate information transfer capacity in a given network (Rubinov and Sporns, 2010), it is possible that they can maintain their values across conditions in tandem with large-scale changes in partition structure (of the sort documented here). In this respect, our findings are consistent with prior work by Moussa et al. (2011) that compared modular arrangement of functional networks during viewing of audiovisual movies and during rest. They reported that movie viewing did not significantly impact the magnitude of any whole brain topological network metric as compared to rest. Yet it did impact the structure of modules that contained primary auditory cortex proper (TTG, TTS): during the resting state, auditory cortex regions clustered in a module that contained somatosensory cortices bilaterally, whereas during multisensory stimulation auditory regions clustered in a module confined to bilateral lateral temporal cortices. The manipulation we used here is clearly of a different sort, as it did not manipulate stimulus features, presenting the exact same sensory information. This shows that sensory features are not the only potential mediator of such organizational effects. Macro-scale network flexibility can also derive from higher-level manipulations (Spreng et al., 2010; Vatansever et al., 2015).

Overall, the network-partitioning procedures showed that reviewing an audiovisual narrative introduces macro-scale changes in the structure of network partitions. At the same time, the distribution of these changes was far from uniform across the brain. Bilateral temporal and inferior frontal regions showed relative inconsistency in their within-module connectivity. By contrast, DMN regions showed a much higher consistency. This dissociation between relatively stable DMN connectivity on the one hand and relatively instable lateral temporal and inferior frontal regions on the other is similar to what we previously found in examining connectivity during listening to auditory tonal series that differ in regularity (Andric and Hasson, 2015). It suggests a general capacity for reorganization of connectivity in perisylvian regions. The relative stability (lower instability) of DMN connectivity here, however, does not mean it is unperturbed by task or executive demands. For instance, Alavash et al (2016) identified differing PCC modular-connectivity to other brain areas under visuo-spatial and speech identification dual-tasks, whereas Lin et al (2016) found this area's degrees during rest associated with later visual task performance. But in the current passive perception task, nodes within this network showed more systematic connectivity profiles.

C. Implications for context-dependent connectivity of lateral temporal and inferior frontal regions

The relative flexibility of functional (and structural) connectivity in the human brain is a matter of ongoing research and emerging debate (see Andric and Hasson, 2015; Hasson et al., 2016 for detailed discussion). Our results highlight the relative flexibility for network-level reorganization in lateral temporal and inferior frontal regions, in the context of language comprehension. This flexibility is likely because these regions are involved in much more than simply coding for phonetic, syllabic or semantic information communicated by language. Language relies on diverse cognitive processes. These include control (Fedorenko, 2014), mentalizing about the beliefs of others (Gallagher and Frith, 2003; Gallagher et al., 2000; Mar, 2011), interfaces with sensorimotor systems (Arbib, 2005; Pulvermüller, 2005; Rizzolatti and Arbib, 1998) as well as memory retrieval (Gerrig and McKoon, 2001) and memory encoding (Hasson et al., 2007). There have also been multiple demonstrations of co-activation between lateral temporal and inferior frontal regions with other functional networks (see Hasson and Egidi, 2015 for discussion). Thus, our findings support that notion that even though frontal and lateral-temporal regions form a neuroanatomical network (Dick and Tremblay, 2012; Friederici, 2009), these anatomical connections do not constrain substantial functional reorganization of these regions' connectivity.

As mentioned in the Introduction, areas implicated in language comprehension can modulate their connectivity with other brain regions based on input familiarity (Müller et al., 2013; Wilkins et al., 2014), input regularity (Andric and Hasson, 2015) or a story's content (Chow et al., 2014). Our study highlights that such reorganization of lateral-temporal regions is scale dependent, showing three complementary features: i) maintenance of nodal (single-voxel) time series features, ii) while accompanied by local connectivity changes in perisylvian regions (of the left hemisphere) and iii) macro-scale modular reorganization at the whole brain level.

With respect to the notion of a fixed language network, the organizational flexibility we identified for lateral temporal and inferior frontal regions raises a question about the extent to which the neuroanatomical connections between these regions actually constrain functional connectivity patterns during online processing. Put differently: how useful is it to talk about "a language network" in a functional sense, if the regions that comprise that network show transient organization during language comprehension? Certainly, these regions exhibit a strong tendency for co-activation and clustering (as we showed in the first viewing). But their connectivity with the rest of the brain is nonetheless strongly context dependent, as evident in our network-level analyses: they change their mean connectivity strength vs. other brain regions, as well as their clustering within specific modules.

Finally, our findings highlight the strong manner in which different analytic methods can shed different sorts of light on language processing. Methods such as intra-subject correlation capture a "local," univariate, similarity metric, and given that it

is aimed at capturing significant similarity in activity for an external input (across viewings) it is a short step to speak about these brain regions as involved in bottom-up processing of an input. However, multivariate analyses, based on pairwise connectivity or network partitioning, address network organizations that can still differ across contexts/conditions, even when the local activity in some nodes does not change with context or repetition. This could indicate, e.g., different organization of efferent or afferent connectivity of these nodes. The network-level changes we described in the current study might be due to memory recall processes and top-down interventions. By any means, these changes in network organization found for lateral-temporal regions and low-level sensory regions indicate that these are not operating under a strict, "informationally encapsulated" regime. This suggests that future work quantifying context-dependent responses may gain much insight from the use of complex network measures, in addition to more typical univariate approaches.

D. The role of prior knowledge in organizing brain activity

In the current study, we found a relatively weak role for systems that have been previously implicated in bridging online language comprehension and long-term knowledge. In View2, participants again watched narratives they had just seen. The narrative content was thus already familiar, so systems implicated in integration of long-term knowledge in the context of language comprehension could have been expected to play a larger role. For instance, prior knowledge of a content domain has been linked with weaker connectivity between vmPFC and the hippocampus during encoding (van Kesteren et al., 2010), and more generally, vmPFC has been linked to application of schema-based information (Ghosh and Gilboa, 2014). In addition, several paradigms have examined the integration of sentence-level information given the presence or absence of disambiguating information. Interestingly, these studies have typically implicated the DMN as being involved in more fluent information integration, seen in higher activity or connectivity when sentences are presented in a disambiguated context (Ames et al., 2015; Martín-Loeches et al., 2008; Smirnov et al., 2014). But our effects here differ from those. We found stronger evidence for mean connectivity change (and within module connectivity arrangement) for lateral temporal regions than for the DMN or vmPFV.

One possibility is that complete stimulus repetition of the sort we used, especially within a short temporal interval such as the one implemented here, simply does not necessitate reliance on long-term memory systems to aid comprehension. As opposed to the manipulations used in the aforementioned studies, our stimuli were simple and easily understood from the outset. They did not rely on details already established during the first viewing. Furthermore, cognitive psychologists have long noted that the relative impact of long-term knowledge on re-experiencing a narrative is more limited than one might expect, leading to phenomenon such as anomalous suspense (where individuals enjoy watching suspenseful movies whose ending they already know). Gerrig (1997) suggested that this anomaly "does not rely on accidental retrieval failure. Rather, it reflects a systematic failure of memory processes to produce relevant knowledge as a narrative unfolds". This cognitive account still requires investigation at a neurobiological level. But it suggests circumstances, be they due to an enjoyment of suspense or other reasons, in which there is a disconnect between systems involved in 'local' textual parsing, e.g., of a single sentence, and those of long-term memory.

E. Limitations and future directions

A limitation of the current work was the relatives sparseness of the behavioral data, which due to a relatively limited range may have limited our ability to link changes in connectivity to a direct measure of comprehension. Nonetheless, ISC, due to its definition, may be an alternative, implicit measure of a person's monitoring of exogenous stimuli, and future work may be able to directly link ISC to indices of explicit behavior. In addition, our current study only touched on the multitude of approaches for characterizing contextual effects on network reconfiguration. The degree to which specific nodes maintain allegiance within the same module (flexibility; e.g., Bassett et al., 2011) could be used to characterize change, as could methods for characterizing reorganization at the "mid-level" of modules, for instance, characterizing similarity in nodal composition of modules across contexts (e.g., Alavash et al., 2015). An additional single-voxel metric that could be evaluated in future work is characterizing the connectivity change of each node in terms of movement within the 2-Dimensional space defined by Guimera and Amaral (2005), based on inter- and intra-module connections and movement within this space across tasks or in relation to individual differences.

We studied functional connectivity patterns that reflect three types of processes. First, some synchronization, such as that between bilateral auditory cortices, may reflect a relatively direct result of sensitivity to sensory-driven features. A second form of synchronicity my reflect higher level processing of the stimulus features that does not track any specific low-level feature, and may be relatively weakly time-locked. (These two types define 'externally oriented' systems; cf. Golland et al., 2007). Finally, some synchronization may reflect connectivity in systems that are completely stimulus-independent ("intrinsic"). Because we did not use a task-based design we did not attempt to partial-out from the signal the impact of the external sensory driver. In this sense, our work differs form prior studies that used task-based design and sought to remove the direct impact of task on connectivity prior to such analyses (e.g., Alavash et al., 2015). Future work with naturalistic stimuli could consider including as regressors time-series sampled from low-level sensory regions (as a proxy for the timeline of external stimulation),

F. Summary

We find that brain activity reorganizes when people process the same audiovisual narratives a second time. This reorganization exhibits complexity, evident at multiple spatial scales. At the most local level, occipital and temporal brain systems involved in sensory processing maintain a similar temporal activation profile. Pairwise interactions at this level, however, already show connectivity strength changes in left temporal areas. At the level of the whole brain, there is rearrangement of modular structure, with lateral temporal and inferior frontal regions showing strong shifts in their within-module connectivity. In this way, our findings show that repetition associates with diverse network-level connectivity changes on multiple scales, including those regions considered core to language processing.

References

1. Achard, S., Salvador, R., Whitcher, B., Suckling, J., Bullmore, E., 2006. A resilient, low-frequency, small-world human brain functional network with highly connected association cortical hubs. J. Neurosci. 26, 63–72. doi:10.1523/JNEUROSCI.3874-05.2006
2. Alavash, M., Hilgetag, C.C., Thiel, C.M., Gießing, C., 2015. Persistency and flexibility of complex brain networks underlie dual-task interference. Hum. Brain Mapp. 36, 3542–3562. doi:10.1002/hbm.22861
3. Alavash, M., Thiel, C.M., Gießing, C., 2016. Dynamic coupling of complex brain networks and dual-task behavior. Neuroimage 129, 233–246. doi:10.1016/j.neuroimage.2016.01.028
4. Alexander-Bloch, A.F., Gogtay, N., Meunier, D., Birn, R., Clasen, L., Lalonde, F., Lenroot, R., Giedd, J., Bullmore, E.T., 2010. Disrupted modularity and local connectivity of brain functional networks in childhood-onset schizophrenia. Front. Syst. Neurosci. 4, 147. doi:10.3389/fnsys.2010.00147
5. Ames, D.L., Honey, C.J., Chow, M.A., Todorov, A., Hasson, U., 2015. Contextual Alignment of Cognitive and Neural Dynamics. J. Cogn. Neurosci. 27, 655–664. doi:10.1162/jocn_a_00728
6. Andersson, J.L.R., Jenkinson, M., Smith, S., 2007. Non-linear registration aka Spatial normalisation FMRIB Technial Report TR07JA2. In Pract. 22.
7. Andric, M., Hasson, U., 2015. Global features of functional brain networks change with contextual disorder. Neuroimage 117, 103–113. doi:10.1016/j.neuroimage.2015.05.025
8. Andric, M., Small, S.L., 2012. Gesture's Neural Language. Front. Psychol. 3, 99. doi:10.3389/fpsyg.2012.00099
9. Andric, M., Solodkin, A., Buccino, G., Goldin-Meadow, S., Rizzolatti, G., Small, S.L., 2013. Brain function overlaps when people observe emblems, speech, and grasping. Neuropsychologia 51, 1619–29. doi:10.1016/j.neuropsychologia.2013.03.022
10. Antrobus, J., 1968. Information theory and stimulus-independent thought. Br. J. Psychol. 59, 423–430.
11. Arbib, M.A., 2005. From monkey-like action recognition to human language : An evolutionary framework for neurolinguistics. Behav. Brain Sci. 28, 105–167.
12. Argall, B.D., Saad, Z.S., Beauchamp, M.S., 2006. Simplified Intersubject Averaging on the Cortical Surface Using SUMA. Hum. Brain Mapp. 27, 14 –27. doi:10.1002/hbm.20158
13. Bassett, D.S., Meyer-Lindenberg, A., Achard, S., Duke, T., Bullmore, E., 2006. Adaptive reconfiguration of fractal small-world human brain functional networks. Proc. Natl. Acad. Sci. U. S. A. 103, 19518–23. doi:10.1073/pnas.0606005103
14. Bassett, D.S., Porter, M. a, Wymbs, N.F., Grafton, S.T., Carlson, J.M., Mucha, P.J., 2013. Robust detection of dynamic community structure in networks. Chaos 23, 013142. doi:10.1063/1.4790830
15. Bassett, D.S., Wymbs, N.F., Porter, M. a, Mucha, P.J., Carlson, J.M., Grafton, S.T., 2011. Dynamic reconfiguration of human brain networks during learning. Proc. Natl. Acad. Sci. U. S. A. 108, 7641–6. doi:10.1073/pnas.1018985108
16. Bernstein, L.E., Liebenthal, E., 2014. Neural pathways for visual speech perception. Front. Neurosci. 8, 1–18. doi:10.3389/fnins.2014.00386
17. Blondel, V.D., Guillaume, J.-L., Lambiotte, R., Lefebvre, E., 2008. Fast unfolding of communities in large networks. J. Stat. Mech. Theory Exp. 2008, P10008. doi:10.1088/1742-5468/2008/10/P10008
18. Boldt, R., Malinen, S., Seppä, M., Tikka, P., Savolainen, P., Hari, R., Carlson, S., 2013. Listening to an Audio Drama Activates Two Processing Networks, One for All Sounds, Another Exclusively for Speech. PLoS One 8, 1–10. doi:10.1371/journal.pone.0064489
19. Brázdil, M., Mikl, M., Marecek, R., Krupa, P., Rektor, I., 2007. Effective connectivity in target stimulus processing: a dynamic causal modeling study of visual oddball task. Neuroimage 35, 827–35. doi:10.1016/j.neuroimage.2006.12.020
20. Brunet, N.M., Bosman, C.A., Vinck, M., Roberts, M., Oostenveld, R., Desimone, R., De Weerd, P., Fries, P., 2014. Stimulus repetition modulates gamma-band synchronization in primate visual cortex. Proc. Natl. Acad. Sci. 111, 3626–3631. doi:10.1073/pnas.1309714111
21. Chow, H.M., Mar, R.A., Xu, Y., Liu, S., Wagage, S., Braun, A.R., 2014. Embodied Comprehension of Stories : Interactions between Language Regions and Modality-specific Neural Systems. J. Cogn. Neurosci. 26, 279–295. doi:10.1162/jocn
22. Cole, M.W., Pathak, S., Schneider, W., 2010. NeuroImage Identifying the brain's most globally connected regions. Neuroimage 49, 3132–3148. doi:10.1016/j.neuroimage.2009.11.001
23. Cox, R.W., 1996. AFNI: software for analysis and visualization of functional magnetic resonance neuroimages. Comput. Biomed. Res. 29, 162–173. doi:10.1006/cbmr.1996.0014
24. Dale, A.M., Fischl, B., Sereno, M.I., 1999. Cortical surface-based analysis. I. Segmentation and surface reconstruction. Neuroimage 9, 179–194. doi:10.1006/nimg.1998.0395
25. den Ouden, H.E.M., Daunizeau, J., Roiser, J., Friston, K.J., Stephan, K.E., 2010. Striatal prediction error modulates cortical coupling. J. Neurosci. 30, 3210–9. doi:10.1523/JNEUROSCI.4458-09.2010
26. Dick, A.S., Tremblay, P., 2012. Beyond the arcuate fasciculus: consensus and controversy in the connectional anatomy of language. Brain 135, 3529–50. doi:10.1093/brain/aws222
27. Eklund, A., Nichols, T.E., Knutsson, H., 2016. Cluster failure : Why fMRI inferences for spatial extent have inflated false-positive rates. doi:10.1073/pnas.1602413113
28. Ewbank, M.P., Henson, R.N., Rowe, J.B., Stoyanova, R.S., Calder, A.J., 2013. Different neural mechanisms within occipitotemporal cortex underlie repetition suppression across same and different-size faces. Cereb. Cortex 23, 1073–1084. doi:10.1093/cercor/bhs070
29. Ewbank, M.P., Lawson, R.P., Henson, R.N., Rowe, J.B., Passamonti, L., Calder, A.J., 2011. Changes in "Top-Down" Connectivity Underlie Repetition Suppression in the Ventral Visual Pathway. J. Neurosci. 31, 5635–5642. doi:10.1523/JNEUROSCI.5013-10.2011
30. Fair, D.A., Schlaggar, B.L., Cohen, A.L., Miezin, F.M., Dosenbach, N.U.F., Wenger, K.K., Fox, M.D., Snyder, A.Z., Raichle, M.E., Petersen, S.E., 2007. A method for using blocked and event-related fMRI data to study "resting state" functional connectivity. Neuroimage 35, 396–405. doi:10.1016/j.neuroimage.2006.11.051
31. Fedorenko, E., 2014. The role of domain-general cognitive control in language comprehension. Front. Psychol. 5, 335. doi:10.3389/fpsyg.2014.00335
32. Ferstl, E.C., Neumann, J., Bogler, C., von Cramon, D.Y., 2008. The extended language network: a meta-analysis of neuroimaging studies on text comprehension. Hum. Brain Mapp. 29, 581–93. doi:10.1002/hbm.20422
33. Fischl, B., Liu, A., Dale, A.M., 2001. Automated manifold surgery: constructing geometrically accurate and topologically correct models of the human cerebral cortex. {IEEE} Trans Med Imaging 20, 70–80. doi:10.1109/42.906426
34. Fischl, B., Salat, D.H., Busa, E., Albert, M., Dieterich, M., Haselgrove, C., van der Kouwe, A., Killiany, R., Kennedy, D., Klaveness, S., Montillo, A., Makris, N., Rosen, B., Dale, A.M., 2002. Whole brain segmentation: automated labeling of neuroanatomical structures in the human brain. Neuron 33, 341–55.
35. Fischl, B., Salat, D.H., van der Kouwe, A.J., Makris, N., Segonne, F., Quinn, B.T., Dale, A.M., 2004. Sequence-independent segmentation of magnetic resonance images. Neuroimage 23 Suppl 1, S69–84. doi:10.1016/j.neuroimage.2004.07.016
36. Fischl, B., Sereno, M.I., Dale, A.M., 1999a. Cortical surface-based analysis. {II}: Inflation, flattening, and a surface-based coordinate system. Neuroimage 9, 195–207. doi:10.1006/nimg.1998.0396
37. Fischl, B., Sereno, M.I., Tootell, R.B.H., Dale, A.M., 1999b. High-resolution inter-subject averaging and a coordinate system for the cortical surface. Hum. Brain Mapp. 8, 272–284.
38. Fornito, A., Zalesky, A., Bullmore, E.T., 2010. Network scaling effects in graph analytic studies of human resting-state FMRI data. Front. Syst. Neurosci. 4, 22. doi:10.3389/fnsys.2010.00022
39. Friederici, A.D., 2009. Pathways to language: fiber tracts in the human brain. Trends Cogn. Sci. 13, 175–181. doi:10.1016/j.tics.2009.01.001

40. Gallagher, H.L., Frith, C.D., 2003. Functional imaging of "theory of mind." Trends Cogn. Sci. 7, 77–83. doi:10.1016/S1364-6613(02)00025-6
41. Gallagher, H.L., Happé, F., Brunswick, N., Fletcher, P.C., Frith, U., Frith, C.D., 2000. Reading the mind in cartoons and stories: An fMRI study of "theory of mind" in verbal and nonverbal tasks. Neuropsychologia 38, 11–21. doi:10.1016/S0028-3932(99)00053-6
42. Garrido, M.I., Kilner, J.M., Kiebel, S.J., Friston, K.J., 2009. Dynamic Causal Modeling of the Response to Frequency Deviants 2620–2631. doi:10.1152/jn.90291.2008.
43. Gerrig, R.J., 1989. Suspense in the absence of uncertainty. J. Mem. Lang. 28, 633–648. doi:10.1016/0749-596X(89)90001-6
44. Gerrig, R.J., McKoon, G., 2001. Memory Processes and Experiential Continuity. Psychol. Sci. 12, 81–85. doi:10.1111/1467-9280.00314
45. Ghosh, V.E., Gilboa, A., 2014. What is a memory schema? A historical perspective on current neuroscience literature. Neuropsychologia 53, 104–114. doi:10.1016/j.neuropsychologia.2013.11.010
46. Ginestet, C.E., Nichols, T.E., Bullmore, E.T., Simmons, A., 2011. Brain network analysis: separating cost from topology using cost-integration. PLoS One 6, e21570. doi:10.1371/journal.pone.0021570
47. Glover, G.H., Li, T.Q., Ress, D., 2000. Image-based method for retrospective correction of physiological motion effects in fMRI: RETROICOR. Magn. Reson. Med. 44, 162–7.
48. Golland, Y., Bentin, S., Gelbard, H., Benjamini, Y., Heller, R., Nir, Y., Hasson, U., Malach, R., 2007. Extrinsic and intrinsic systems in the posterior cortex of the human brain revealed during natural sensory stimulation. Cereb. Cortex 17, 766–77. doi:10.1093/cercor/bhk030
49. Grill-Spector, K., Henson, R., Martin, A., 2006. Repetition and the brain: neural models of stimulus-specific effects. Trends Cogn. Sci. 10, 14–23. doi:10.1016/j.tics.2005.11.006
50. Guimera, R., Amaral, L.A.N., 2005. Functional cartography of complex metabolic networks. Nature 433, 895–900. doi:10.1038/nature03286.1.
51. Hampson, M., Driesen, N.R., Skudlarski, P., Gore, J.C., Constable, R.T., 2006. Brain connectivity related to working memory performance. J. Neurosci. 26, 13338–43. doi:10.1523/JNEUROSCI.3408-06.2006
52. Hasson, U., Andric, M., Atilgan, H., Collignon, O., 2016. Congenital blindness is associated with large-scale reorganization of anatomical networks. Neuroimage 128, 362–372. doi:10.1016/j.neuroimage.2015.12.048
53. Hasson, U., Egidi, G., 2015. What are naturalistic comprehension paradigms teaching us about language?, in: Willems, R. (Ed.), Cognitive Neuroscience of Natural Language Use. Cambridge University Press, pp. 228–255.
54. Hasson, U., Nusbaum, H.C., Small, S.L., 2009. Task-dependent organization of brain regions active during rest. Proc. Natl. Acad. Sci. U. S. A. 106, 10841–6. doi:10.1073/pnas.0903253106
55. Hasson, U., Nusbaum, H.C., Small, S.L., 2007. Brain networks subserving the extraction of sentence information and its encoding to memory. Cereb. Cortex 17, 2899–913. doi:10.1093/cercor/bhm016
56. Hawco, C., Lepage, M., 2014. Overlapping patterns of neural activity for different forms of novelty in fMRI. Front. Hum. Neurosci. 8, 699. doi:10.3389/fnhum.2014.00699
57. Hayasaka, S., Laurienti, P.J., 2010. Comparison of characteristics between region-and voxel-based network analyses in resting-state fMRI data. Neuroimage 50, 499–508. doi:10.1016/j.neuroimage.2009.12.051
58. Hickok, G., Poeppel, D., 2007. The cortical organization of speech processing. Nature 8, 393–402.
59. Jaccard, P., 1901. Étude comparative de la distribution florale dans une portion des Alpes et des Jura. Bull. del la Société Vaudoise des Sci. Nat. 37, 547–579. doi:http://dx.doi.org/10.5169/seals-266450
60. Jenkinson, M., Bannister, P., Brady, M., Smith, S., 2002. Improved optimization for the robust and accurate linear registration and motion correction of brain images. Neuroimage 17, 825–841. doi:10.1016/S1053-8119(02)91132-8
61. Jenkinson, M., Smith, S., 2001. A global optimisation method for robust affine registration of brain images. Med. Image Anal. 5, 143–156. doi:10.1016/S1361-8415(01)00036-6
62. Kafkas, A., Montaldi, D., 2015. Striatal and midbrain connectivity with the hippocampus selectively boosts memory for contextual novelty. Hippocampus 12, 1–12. doi:10.1002/hipo.22434
63. Kelly, a M.C., Uddin, L.Q., Biswal, B.B., Castellanos, F.X., Milham, M.P., 2008. Competition between functional brain networks mediates behavioral variability. Neuroimage 39, 527–37. doi:10.1016/j.neuroimage.2007.08.008
64. Lancichinetti, A., Fortunato, S., 2012. Consensus clustering in complex networks. Sci. Rep. 2, 336. doi:10.1038/srep00336
65. Levin, D.N., Uftring, S.J., 2001. Detecting Brain Activation in FMRI Data without Prior Knowledge of Mental Event Timing. Methods 160, 153–160. doi:10.1006/nimg.2000.0663
66. Liebenthal, E., Ellingson, M.L., Spanaki, M. V, Prieto, T.E., Ropella, K.M., Binder, J.R., 2003. Simultaneous ERP and fMRI of the auditory cortex in a passive oddball paradigm. Neuroimage 19, 1395–1404. doi:10.1016/S1053-8119(03)00228-3
67. Lin, P., Yang, Y., Jovicich, J., De Pisapia, N., Wang, X., Zuo, C.S., Levitt, J.J., 2016. Static and dynamic posterior cingulate cortex nodal topology of default mode network predicts attention task performance. Brain Imaging Behav. 10, 212–225. doi:10.1007/s11682-015-9384-6
68. Mainieri, A.G., Heim, S., Straube, B., Binkofski, F., Kircher, T., 2013. Differential role of the Mentalizing and the Mirror Neuron system in the imitation of communicative gestures. Neuroimage 81, 294–305. doi:10.1016/j.neuroimage.2013.05.021
69. Mar, R. a, 2011. The neural bases of social cognition and story comprehension. Annu. Rev. Psychol. 62, 103–34. doi:10.1146/annurev-psych-120709-145406
70. Marois, R., Leung, H.C., Gore, J.C., 2000. A stimulus-driven approach to object identity and location processing in the human brain. Neuron 25, 717–728. doi:10.1016/S0896-6273(00)81073-9
71. Martín-Loeches, M., Casado, P., Hernández-Tamames, J. a, Alvarez-Linera, J., 2008. Brain activation in discourse comprehension: a 3t fMRI study. Neuroimage 41, 614–22. doi:10.1016/j.neuroimage.2008.02.047
72. Mashal, N., Solodkin, A., Dick, A.S., Elinor Chen, E., Small, S.L., 2012. A network model of observation and imitation of speech. Front. Psychol. 3, 1–12. doi:10.3389/fpsyg.2012.00084
73. Mennes, M., Kelly, C., Colcombe, S., Castellanos, F.X., Milham, M.P., 2013. The extrinsic and intrinsic functional architectures of the human brain are not equivalent. Cereb. Cortex 23, 223–9. doi:10.1093/cercor/bhs010
74. Meshulam, M., Ramot, M., Harel, M., Kipervasser, S., Andelman, F., Neufeld, M.Y., Kramer, U., Fried, I., Malach, R., 2013. Selectivity of audiovisual ECoG responses revealed under naturalistic stimuli in the human cortex. J. Neurophysiol. 109, 2272–81. doi:10.1152/jn.00474.2012
75. Moussa, M.N., Steen, M.R., Laurienti, P.J., Hayasaka, S., 2012. Consistency of network modules in resting-state FMRI connectome data. PLoS One 7, e44428. doi:10.1371/journal.pone.0044428
76. Moussa, M.N., Vechlekar, C.D., Burdette, J.H., Steen, M.R., Hugenschmidt, C.E., Laurienti, P.J., 2011. Changes in cognitive state alter human functional brain networks. Front. Hum. Neurosci. 5, 83. doi:10.3389/fnhum.2011.00083
77. Müller, N., Keil, J., Obleser, J., Schulz, H., Grunwald, T., Bernays, R.-L., Huppertz, H.-J., Weisz, N., 2013. You can't stop the music: Reduced auditory alpha power and coupling between auditory and memory regions facilitate the illusory perception of music during noise. Neuroimage 79, 383–393. doi:10.1016/j.neuroimage.2013.05.001
78. Oldfield, R.C., 1971. The assessment and analysis of handedness: the Edinburgh inventory. Neuropsychologia 9, 97–113. doi:10.1016/0028-3932(71)90067-4
79. Opitz, B., Rinne, T., Mecklinger, A., von Cramon, D.Y., Schröger, E., 2002. Differential Contribution of Frontal and Temporal Cortices to Auditory Change Detection: fMRI and ERP Results. Neuroimage 15, 167–174. doi:10.1006/nimg.2001.0970
80. Patenaude, B., Smith, S.M., Kennedy, D.N., Jenkinson, M., 2011. A Bayesian model of shape and appearance for subcortical brain segmentation. Neuroimage 56, 907–922. doi:10.1016/j.neuroimage.2011.02.046

81. Peigneux, P., Salmon, E., van der Linden, M., Garraux, G., Aerts, J., Delfiore, G., Degueldre, C., Luxen, a, Orban, G., Franck, G., 2000. The role of lateral occipitotemporal junction and area MT/V5 in the visual analysis of upper-limb postures. Neuroimage 11, 644–655. doi:10.1006/nimg.2000.0578
82. Pulvermüller, F., 2005. Brain mechanisms linking language and action. Nat. Rev. Neurosci. 6, 576–582. doi:10.1038/nrn1706
83. Ranganath, C., Rainer, G., 2003. Cognitive neuroscience: Neural mechanisms for detecting and remembering novel events. Nat. Rev. Neurosci. 4, 193–202. doi:10.1038/nrn1052
84. Rizzolatti, G., Arbib, M.A., 1998. Language within our grasp. TINS 21, 188–194.
85. Rubinov, M., Sporns, O., 2010. NeuroImage Complex network measures of brain connectivity : Uses and interpretations. Neuroimage 52, 1059–1069. doi:10.1016/j.neuroimage.2009.10.003
86. Saad, Z.S., Reynolds, R.C., Argall, B., Japee, S., Cox, R.W., 2004. SUMA: an interface for surface-based intra- and inter-subject analysis with AFNI, in: Biomedical Imaging: Nano to Macro, 2004. IEEE International Symposium on. pp. 1510–1513 Vol. 2.
87. Shervashidze, N., Schweitzer, P., Leeuwen, V., Jan, E., Mehlhorn, K., Borgwardt, K., 2011. Weisfeiler-Lehman graph kernels. J. Mach. Learn. Res. 12, 2539–2561.
88. Skipper, J.I., Wassenhove, V., V., N., H.c, Small, S.L., 2007. Hearing lips and seeing voices: how cortical areas supporting speech production mediate audiovisual speech perception. Cerebr. Cortex 17, 2387–2399.
89. Smirnov, D., Glerean, E., Lahnakoski, J.M., Salmi, J., Jääskeläinen, I.P., Sams, M., Nummenmaa, L., 2014. Fronto-parietal network supports context-dependent speech comprehension. Neuropsychologia 63, 293–303. doi:10.1016/j.neuropsychologia.2014.09.007
90. Smith, S.M., 2002. Fast robust automated brain extraction. Hum. Brain Mapp. 17, 143–155. doi:10.1002/hbm.10062
91. Spreng, R.N., Stevens, W.D., Chamberlain, J.P., Gilmore, A.W., Schacter, D.L., 2010. Default network activity, coupled with the frontoparietal control network, supports goal-directed cognition. Neuroimage 53, 303–317. doi:10.1016/j.neuroimage.2010.06.016
92. Stanley, M.L., Dagenbach, D., Lyday, R.G., Burdette, J.H., Laurienti, P.J., 2014. Changes in global and regional modularity associated with increasing working memory load. Front. Hum. Neurosci. 8, Article 954. doi:10.3389/fnhum.2014.00954
93. Stephens, G.J., Silbert, L.J., Hasson, U., 2010. Speaker-listener neural coupling underlies successful communication. Proc. Natl. Acad. Sci. U. S. A. 107, 14425–30. doi:10.1073/pnas.1008662107
94. Strange, B. a, Duggins, A., Penny, W., Dolan, R.J., Friston, K.J., 2005. Information theory, novelty and hippocampal responses: unpredicted or unpredictable? Neural Netw. 18, 225–30. doi:10.1016/j.neunet.2004.12.004
95. Torta, D.M., Cauda, F., 2011. Different functions in the cingulate cortex, a meta-analytic connectivity modeling study. Neuroimage 56, 2157–2172. doi:10.1016/j.neuroimage.2011.03.066
96. Uftring, S.J., Levin, D.N., 2002. fMRI Activation from Passive Listening to Classical Instrumental Music. Brain Res. 98, 11823–11823.
97. van Kesteren, M.T.R., Fernandez, G., Norris, D.G., Hermans, E.J., 2010. Persistent schema-dependent hippocampal-neocortical connectivity during memory encoding and postencoding rest in humans. Proc. Natl. Acad. Sci. 107, 7550–7555. doi:10.1073/pnas.0914892107
98. Vatansever, D., Menon, X.D.K., Manktelow, A.E., Sahakian, B.J., Stamatakis, E.A., 2015. Default Mode Dynamics for Global Functional Integration 35, 15254–15262. doi:10.1523/JNEUROSCI.2135-15.2015
99. Vega-Pons, S., Avesani, P., Andric, M., Hasson, U., 2014. Classification of inter-subject fMRI data based on graph kernels, in: Pattern Recognition in Neuroimaging, 2014 International Workshop on. pp. 1–4. doi:10.1109/PRNI.2014.6858549
100. Vitz, P.C., 1964. Preferences for Rates of Information Presented By Sequences of Tones. J. Exp. Psychol. 68, 176–83.
101. Ward, J.H., 1963. Hierarchical grouping to optimize an objective function. J. Am. Stat. Assoc. doi:10.1080/01621459.1963.10500845
102. Weisfeiler, B., Lehman, A.A., 1968. A reduction of a graph to a canonical form and an algebra arising during this reduction. Naucho–Technicheskaya Informatsia 2, 12–16.
103. Weissman, D.H., Roberts, K.C., Visscher, K.M., Woldorff, M.G., 2006. The neural bases of momentary lapses in attention. Nat. Neurosci. 9, 971–8. doi:10.1038/nn1727
104. Wilkins, R.W., Hodges, D. a, Laurienti, P.J., Steen, M., Burdette, J.H., 2014. Network Science and the Effects of Music Preference on Functional Brain Connectivity: From Beethoven to Eminem. Sci. Rep. 4, 6130. doi:10.1038/srep06130
105. Winkler, A.M., Ridgway, G.R., Webster, M.A., Smith, S.M., Nichols, T.E., 2014. Permutation inference for the general linear model. Neuroimage 92, 381–397.
106. Yu, C., Zhou, Y., Liu, Y., Jiang, T., Dong, H., Zhang, Y., Walter, M., 2011. Functional segregation of the human cingulate cortex is confirmed by functional connectivity based neuroanatomical parcellation. Neuroimage 54, 2571–2581. doi:10.1016/j.neuroimage.2010.11.018
107. Zalesky, A., Fornito, A., Bullmore, E.T., 2010. Network-based statistic: identifying differences in brain networks. Neuroimage 53, 1197–207. doi:10.1016/j.neuroimage.2010.06.041

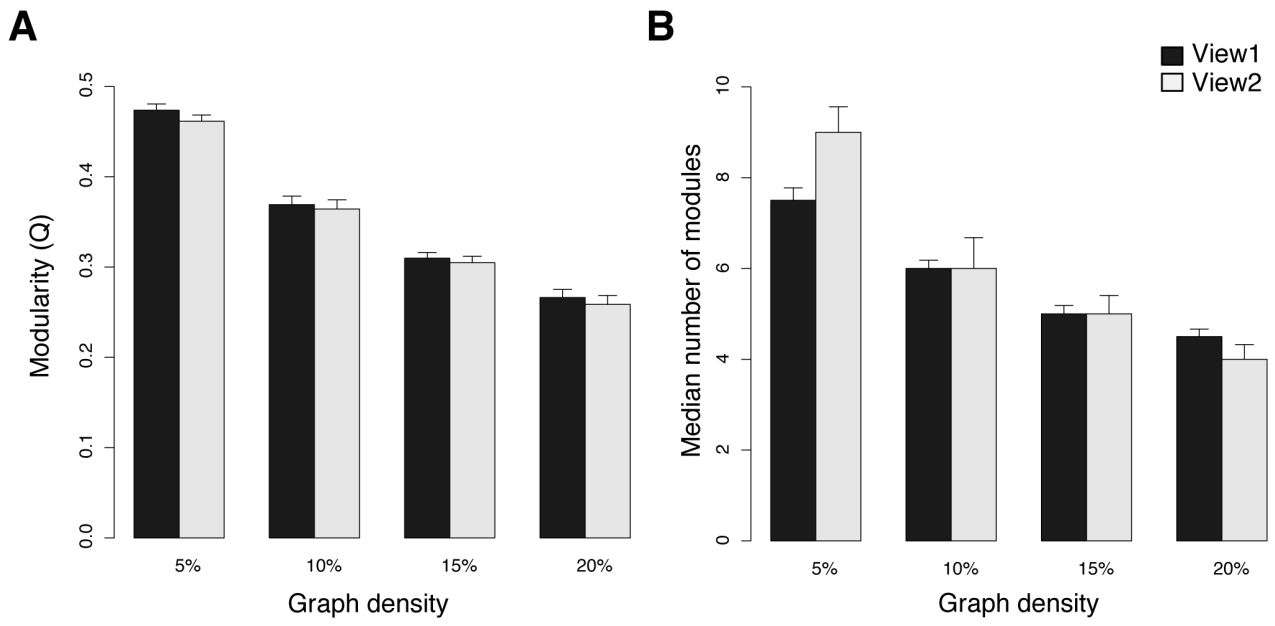

Inline Supplementary Figure 2. Modularity and number of modules do not differ between View1 and View2.

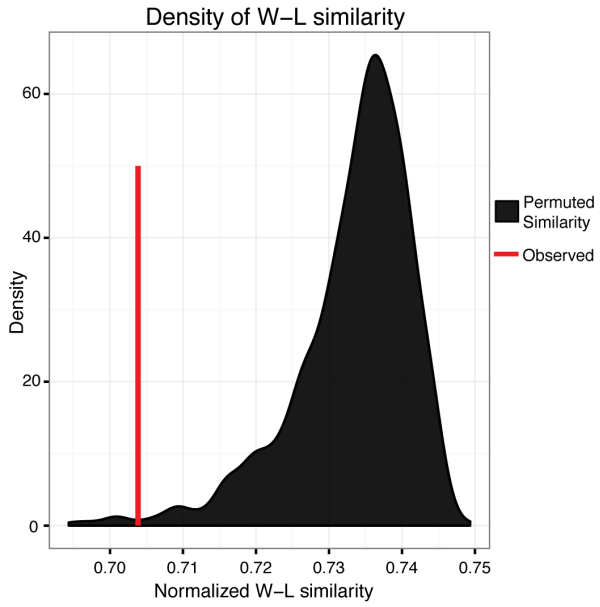

Inline Supplementary Figure 3. Weisfeiler-Lehman based isomorphism test using a graph kernel. The observed similarity value between View1 and View2 (.7038, red line) reflects a level of dissimilarity that is lower than 99% of the values expected by chance, based on a distribution of similarity values from 1000 permutations.

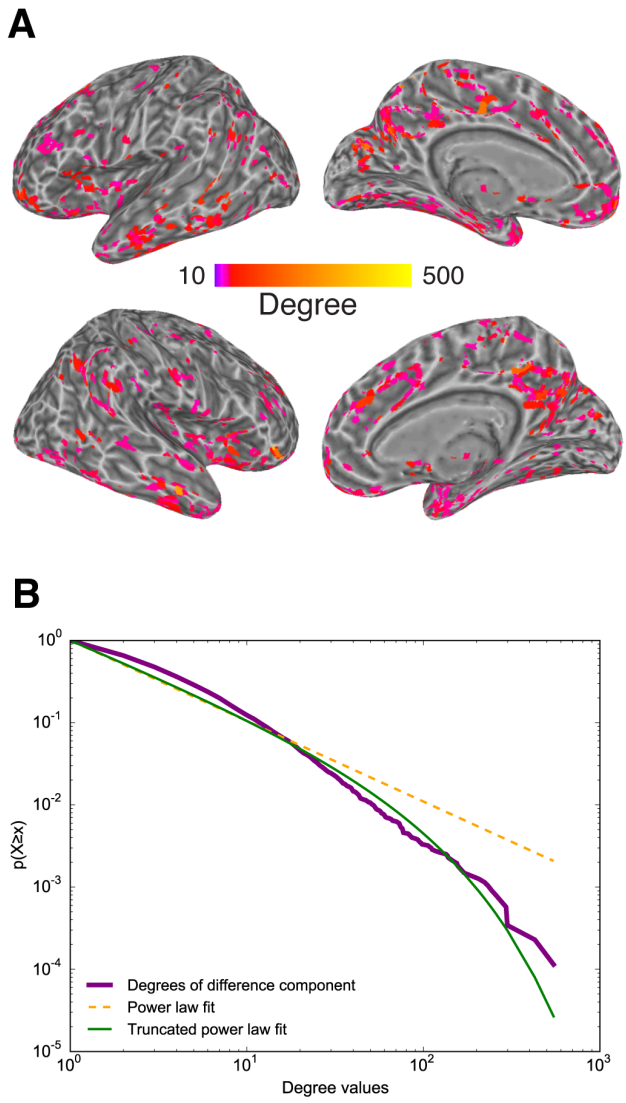

Inline Supplementary Figure 4. Degrees of the difference network.